VTT PUBLICATIONS 704

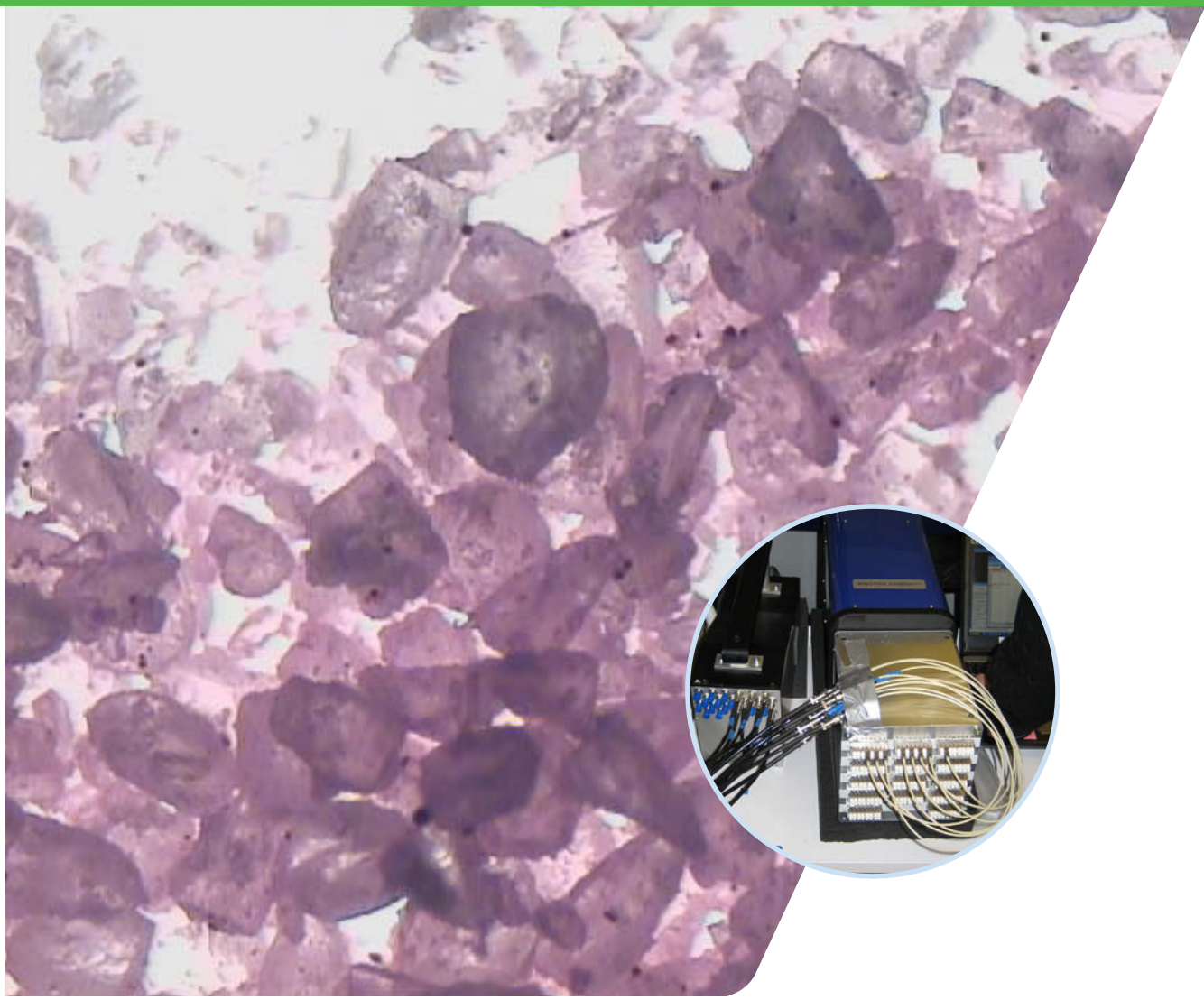

Anne Heikkilä

Multipoint-NIR-measurements in pharmaceutical powder applications

VTT PUBLICATIONS 704

Multipoint-NIR-measurements in pharmaceutical powder applications

Anne Heikkilä

ISBN 978-951-38-7334-9 (soft back ed.)
ISSN 1235-0621 (soft back ed.)

ISBN 978-951-38-7335-6 (URL: http://www.vtt.fi/publications/index.jsp)
ISSN 1455-0849 (URL: http://www.vtt.fi/publications/index.jsp)

JULKAISIJA – UTGIVARE – PUBLISHER

VTT, Vuorimiehentie 5, PL 1000, 02044 VTT
puh. vaihde 020 722 111, faksi 020 722 7001

VTT, Bergsmansvägen 5, PB 1000, 02044 VTT
tel. växel 020 722 111, fax 020 722 7001

VTT Technical Research Centre of Finland, Vuorimiehentie 5, P.O. Box 1000, FI-02044 VTT, Finland
phone internat. +358 20 722 111, fax + 358 20 722 7001

Layout by Tarja Haapalainen

Edita Prima Oy, Helsinki 2009

Anne Heikkilä, Multipoint-NIR-measurements in pharmaceutical powder applications. Espoo 2009. VTT Publications 704. 59 p.

Keywords pharmaceutical powder applications, fluid bed granulation, on-line monitoring, moisture content, mixing end-point, near-infrared spectroscopy, NIR, multichannel spectroscopy, fibre-optic probes, fibre-optic light sources, multipoint-NIR

Abstract

In this paper, multipoint near-infrared (NIR) spectroscopy is used in studying particulate pharmaceutical ingredients and their mixing and granulation processes. Homogeneous mixing of active pharmaceutical ingredients with excipients is essential in getting the correct dosage in the tableting phase. The basic principles of NIR spectroscopy and the associated molecular vibrations are briefly reviewed in the beginning of the work, followed by a summary of typical applications of NIR spectroscopy.

A multipoint NIR measurement system developed at VTT is presented in this work. It consists of a spectral camera with fiber-optic inputs, a fiber-optic light source and twelve fiber-optic probes. The performance of the system in the laboratory is thoroughly reported, including signal-to-noise ratio, stability and probe-to-probe variability. The system was also tested in a fluidized bed granulator at Helsinki University. Eight probes were attached in two rows into the granulator, and several granulations were run. The mixing period in the beginning of the granulation process was clearly visible, as well as the changes in the moisture level during liquid spraying and final drying. The study shows that multipoint NIR spectroscopy is a valuable tool in monitoring the granulation process. In particular, it gives information about the macroscopic homogeneity of the fluidized bed.

Foreword

This thesis was made during PAT-KIVA project at VTT Technical Research Centre of Finland (VTT). The project period was from the beginning of 2007 to the end of 2008 where in April the multipoint-NIR device got ready and the testing of prototype made in this thesis started. The measurements of the pharmaceutical process were made during September at the division of pharmaceutical technology of Helsinki University. The PAT-KIVA project was funded by Tekes – the Finnish Funding Agency for Technology and Innovation and several Finnish and international industrial partners.

I would like to express my genuine thanks to my supervisors, Seppo Alanko (University of Oulu) and Janne Paaso (VTT) for their advice, guidance and continuing support.

Furthermore I would like to thank Mr. Hannu Vasama (VTT) for the mechanical design of the probes, Mr. Rauno Mattila (VTT) for the mechanical design of the light source and Mr. Pekka Suopajärvi (VTT) for the optical design of probes and light source. Then I would like to thank the team of process measurement technology, especially team leader Mrs. Mari Tenhunen, for making me feel welcomed. And when the actual in-line measurements were made thanks for Mr. Lauri Kurki for accompanying me.

Contents

1. Introduction

This work deals with near-infrared spectroscopy and its applications concentrating especially on the multipoint measurement aspect. Multipoint measurement gives new challenges to the measurement situation itself. This can be seen when making a measurement with multipoint device the arrangement of the device has to be thought carefully. Furthermore when measuring with multipoint device the amount of data received is multiple compared to a measurement made using a single-point system. This data amount makes the data analysis more challenging especially in on-line process measurements.

Near-infrared area is a part of the electromagnetic spectrum. It is situated inside the infrared area which is situated between visible light and radio waves [1]. Near-infrared may be used in overtone and combination vibration [2]. When looking at the near-infrared equipments there are plenty to choose from. Four basic components, detector unit, the dispersive component, the sample or process interface and the illumination unit, can be combined to form different equipments [3]. This variety of devices enables wide field of applications.

In this thesis, multipoint-NIR-measurement prototype is used to make the measurements. The first goal is to test the equipment by making performance tests. Before this, the multipoint-NIR-measurement prototype used is described in this thesis. Then the laboratory calibration sets are made using three different powder mixes: caffeine and lactose, ibuprofen and two different size of lactose. Finally the on-line-measurements are made with pharmaceutical powders in fluid-bed granulator. These granulated powders are caffeine and lactose. There is some publications where the measurements made with NIR in the fluid-bed granulator before [4], but none of these are like the measurements made in this thesis.

2. NIR spectroscopy

In this chapter, the basic principles of near infrared spectroscopy are presented as well as some applications.

2.1 Basic principles

The spectral area that this work is concentrated on is called “near infrared” and this area, as we can see in Figure 1, is situated inside the infrared area which exists between visible light and radio waves. Figure 1 describes how we divide the range of electromagnetic spectrum and it also helps us to absolutely identify a position or range within the spectrum.

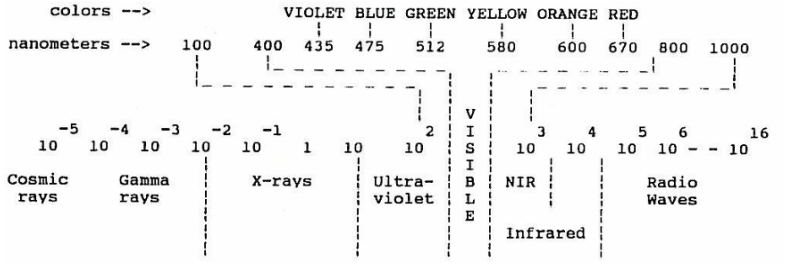

Figure 1. Diagram that names the different regions of the spectrum [1]. Note that the unit is nanometre.

The far infrared may be used for rotational spectroscopy [5], mid infrared may be used to study the rotational-vibrational structure [2] and the near infrared may be used in studying overtone and combination vibrations [2]. It is good to keep in mind that these limits are not strict. Infrared spectroscopy is based on the idea that different molecules have specific frequencies at which they rotate or vibrate.

The near infrared spectroscopy is focused on the molecular overtone and combination vibrations, see for example reference [3] and references there in.

2.2 Molecular vibrations

Next presentation follows the structure of [6]. In the case of an ideal harmonic oscillator, the potential energy V can be written in the following form

$$V = \frac{1}{2}k(r - r_e) = \frac{1}{2}kx^2,$$

where k is the force constant of the bond, x is the displacement coordinate, r and r_e are the internuclear and the equilibrium internuclear distance. Picture of this potential energy can be seen in Figure 2.

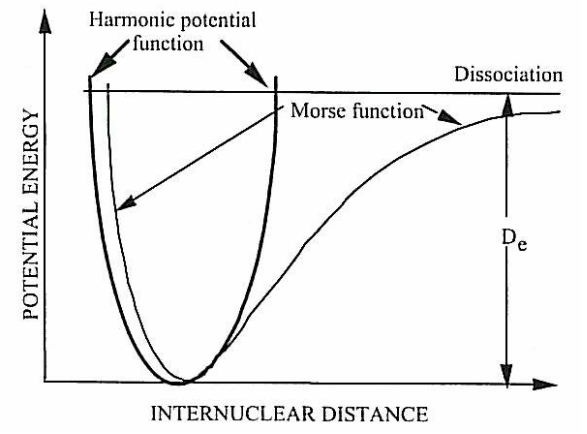

Figure 2. Harmonic and anharmonic potential functions for a diatomic oscillator [6].

The vibrational frequency for the diatomic oscillator is

$$\nu = \frac{1}{2\pi}\sqrt{\frac{k}{\mu}},$$

where μ is the reduced molecular mass, more precisely $\mu = mM/(m+M)$, where m and M are the masses of the two nuclei.

We know from the quantum mechanical approach that the vibrational energy can only get certain discrete values. These values are called energy levels. For our harmonic oscillator these energy levels can be written as

$$E_{vib} = h\nu(v + \frac{1}{2}),$$

where ν is the vibrational frequency defined above, h is the Planck's constant and v is the vibrational quantum number. Note that v can only have integer values 0, 1, 2, … .

The energy levels, in wavenumber units (cm^{-1}), corresponding to different levels of v can be written as

$$G(v) = \frac{E_{vib}}{hc} = \bar{\nu}(v + \frac{1}{2}),$$

where $\bar{\nu}$ is the wavenumber of the vibrational transition. In the quantum mechanical harmonic oscillator there is a restriction to the vibrational quantum number: it can change only by one unit (see Figure 3). Therefore transitions are allowed only if

$$\Delta v = \pm 1 .$$

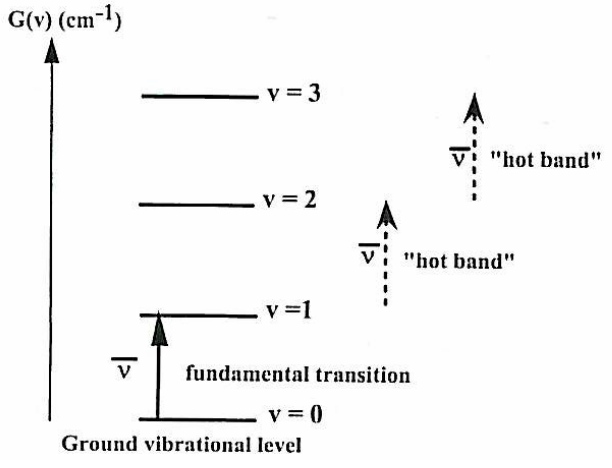

Figure 3. Vibrational energy levels of the harmonic oscillator [6].

Because of the Boltzmann distribution most molecules are at the ground vibrational level $v = 0$ at room temperature. Hence the fundamental transition $v = 0 \rightarrow v = 1$ dominates the infrared absorption spectrum. Most of the infrared absorptions of interest to a chemical spectroscopist happen due to the fundamental transitions. The other transitions such as $v = 1 \rightarrow v = 2$, $v = 2 \rightarrow v = 3$ …, are called "hot bands". This name is given due to the fact that vibrational excited levels are relatively low populated and increasing the temperature will increase the population, and, thus, the intensity of the bands.

As one can imagine, real molecules are not ideal oscillators. This causes a couple of things to happen. First one is that unlike in the ideal case the vibrational energy levels are not equally spaced. This effect is called mechanical anharmonicity and is caused by the higher terms in the potential-energy expression:

$$V = \frac{1}{2}kx^2 + k'x^3 + \ldots,$$

where $k' << k$. This also affects the energy level (cm^{-1}), which can now be written as

$$G(v) = \bar{\nu}(v + \frac{1}{2}) - \chi_e \bar{\nu}(v + \frac{1}{2})^2,$$

where χ_e is the anharmonicity constant. As we can see the higher energy levels are no longer equally spaced.

A function, which is often used as the anharmonic potential function, is called the Morse function and it is written as

$$V = D_e(1 - e^{-\beta x})^2,$$

where β is a constant and D_e is the dissociation energy of the molecule (see Figure 2).

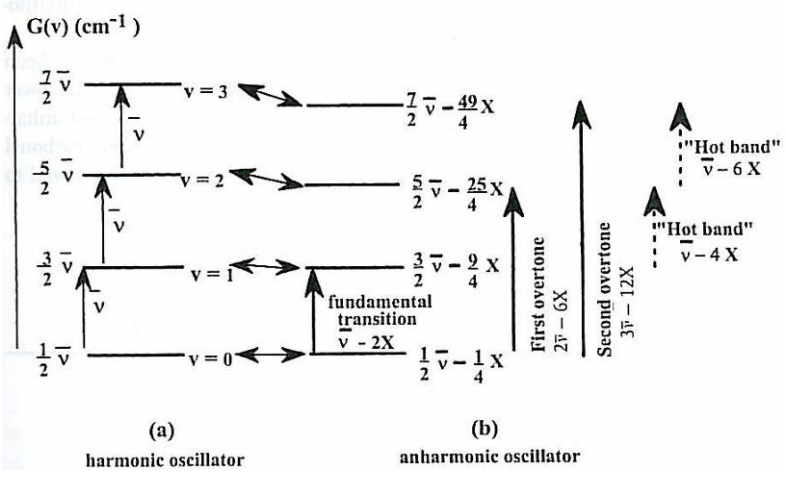

Figure 4. Energy level diagrams and associated transitions [6].

The second difference compared to the ideal harmonic oscillator is that overtone transitions such as $v = 0 \rightarrow v = 2,3,4,...$ become allowed, see Figure 4.

Moving from a diatomic molecule to a polyatomic molecule makes theory a bit more complicated, but it is still easy to keep up. A molecule that has *N* atoms has (3*N*-6) vibrational degrees of freedom (linear molecules have only 3*N*-5). This number tells us the number of fundamental vibrational frequencies of the molecule.

We may make an approximation so that the vibrational molecule is a superposition of (3*N*-6) simple harmonic motions. For example the fundamental frequencies for a nonlinear triatomic molecule, sulphur dioxide SO_2, can be seen in Figure 5, where ν_1 is called the symmetric stretch, ν_2 the bending mode and ν_3 the antisymmetric stretch. Note that v is called the vibrational quantum number and it can only have integer values 0, 1, 2, … .

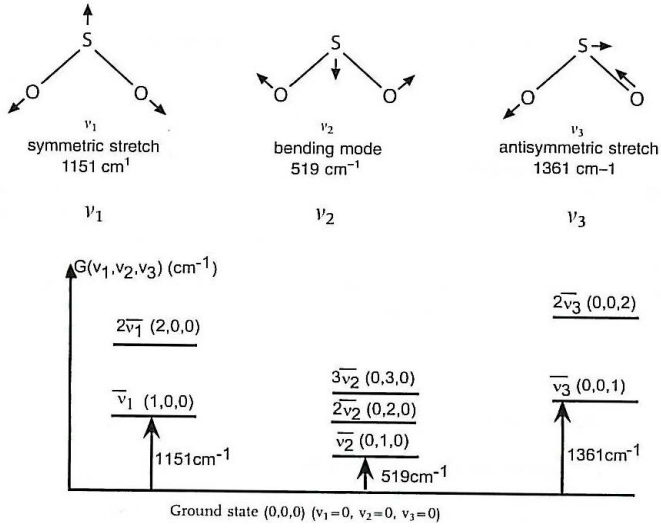

Figure 5. Vibrational energy levels of sulfur dioxide, SO_2 [6].

When the anharmonicity of vibrations is taken into account the overtones and combination vibrations may also occur. As it can be expected the overtones and combination vibrations are much weaker compared to the fundamental bands. There are different names for different types of overtone and combination bands, for example, $\Delta\nu_i = 2$ or $\sum\Delta\nu_i = 2$ are called binary combinations. The binary combinations are stronger that ternary combinations ($\Delta\nu_i = 3$). In Figure 6 we can see an example of the combination levels corresponding to $\nu_1 + \nu_2$, $\nu_1 + \nu_3$ and $\nu_2 + \nu_3$.

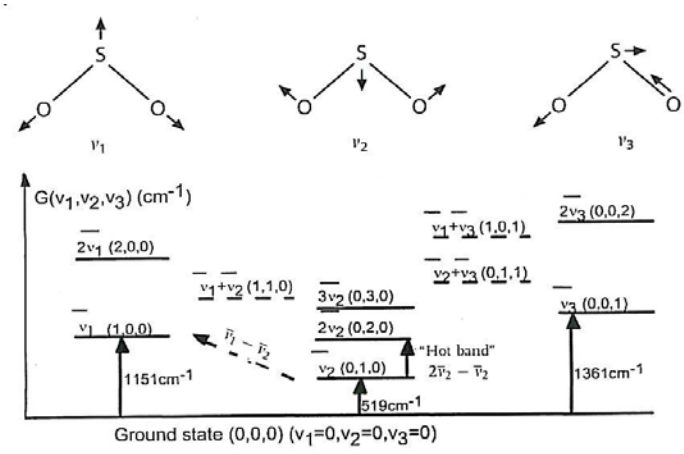

Figure 6. Vibrational energy levels of sulfur dioxide, SO_2 [6].

2.3 About NIR equipment techniques

The NIR spectroscopy equipments are basically constructed from four different components which are the detector unit, the dispersive component, the sample or process interface and the illumination unit [3]. Of course there are multiple possibilities for each of these components.

A particular measurement technique is obtained by combining these four components. The number of different measurement techniques in NIR spectroscopy has increased in the last decades [3]. One example for categorising these is the following: monochromator-based devices, array spectrometers, miniature spectrometers, tuneable filter and discrete filter devices, Hadamard transform spectrometers and spectrometers based on infrared-emitting diodes [7]. An addition to this list should be Fourier transform near-infrared (FT-NIR) spectrometers, which however, works also in other spectral rages than just NIR. Fixed-wavelength devices include for example multi-channel detector based devices and filter wheel devices. Fixed-wavelength means that the measurement is made using 2–8 different wavelengths. In multi-channel detector devices these wavelengths are collected at the same time [8]. The filter wheel devices have a light chopper wheel with different interference filters and the fixed wavelengths are collected to the detector one after another. Instead of fixed-wavelengths there are also continuous spectrum devices which include for example array spectrometers, FT-NIR and spectral cameras. In array spectrometer and spectral

cameras there is one input slit for the light which is then divided to a spectra using a grating and finally it is detected either by array detector or a spectral camera [7]. In the FT-NIR the wavelengths are modulated in the sample.

2.4 Applications

In this chapter some of the applications for NIR spectroscopy is presented. NIR spectroscopy is widely used because it is fast technique and it does not destroy the sample.

Food applications

The most important application of NIR spectroscopy in analysis of food is the quantitative measurement of moisture (O-H stretch first overtone, O-H stretch + O-H deformation), fat (C-H stretch third overtone, 2*N-H stretch + 2*amide I, 2*C-H stretch + 2*C-H deformation + $(CH_2)_n$), protein (C-H stretch third overtone, N-H stretch second overtone, N-H asymmetric stretch + amide II, N-H symmetric stretch + amide II, 2*amide I + amide III) and/or carbohydrate (C-H and O-H bonds) content of food products [9]. Next some of the applications in the food industry is presented.

Beverages

NIR spectroscopy is also used in detecting the sugar content of fruit juice as well as monitoring the moisture content of coffee and tea [10]. The tea analysis field can be divided into two categories. First category is the composition and sensory analysis of teas. This is the qualitative analysis of tea constituents with quality factors like caffeine and total polyphenol content in tea. The second category is separation of tea into either different varieties or categories. Here by different categories we mean e. g. the difference between green, black and Oolong tea [11].

One major application of NIR spectroscopy has been the determination of alcohol content in beer and wine [6]. Calibrations have also been developed for example β-glucan and malt hot water extract, which are monitored during the brewing process [10].

Dairy products

Milk producers must deliver products of high and constant quality dairy products in order to fulfil the consumer requirements. When discussing about milk products quality means a variety of things for example absence of dirt, off-flavours, pathogenic organisms and abnormal number of body cells. The milk analysis can be divided roughly into two different categories: analysis of milk composition and analysis of attributes. In milk quality analysis the things to analyse are for example fat and protein when in composition analysis the searched indicator of a disease can be somatic cell count [11]. This method has been accepted as the world standard for mastitis diagnosis.

Analysis of cheeses' chemical characteristics has been traditionally made by a range of physico-chemical methods which can be labour-intensive and expensive. Recently there have been investigations to use NIR spectroscopy to determine several of cheese parameters. NIRS can be used for moisture control of cream cheese and processed cheese or for the determination of the total solids in fresh cheese to name a few examples [10]. The tricky thing is that various cheeses are made differently and existing calibration sets only work with the cheese type they were originally made for.

Cereal grains and flour

NIR spectroscopy is routinely used in analysis of crops and seed [6]. The use of NIR technology when measuring the moisture content of the wheat and flour is routine nowadays. Likewise one application that is very widely used is the determination of protein content in wheat. This can be a big advantage to farmers in countries where the price of wheat is determined by its protein content. In the year 1995 "The European Grain Network" was brought together in order to standardize the NIR grain testing through the continent. This uniform base for calibration and update of the instruments helps the farmers to eliminate between-instrument variation in their analysis results thus receiving correct grading and the corresponding payment [10]. The detection of contaminants such as weeds or insects is also one important application for the suppliers [11].

Since half of the world's population depends on rice as its main food source unsurprisingly rice is also a widely investigated product [11]. Whiteness and taste are the two most important factors in quality control. Whiteness is not

measured directly from the rice but rather it is measured by determining the bran amount remained on the surface of the milled rice kernel [6].

NIR is also in use at many large bakeries. They monitor the quality of their flour, raw ingredients and the moisture content during the baking process [10].

Other applications

There are also plenty of other applications where NIR is used. The following mentioned applications are to name just a few.

Pasture

NIR spectroscopy is widely used when measuring the chemical composition of pasture. This is because the various morphological components of grasses, for example leaf blade and stem, vary in their nutritive value for ruminants and these differences can be seen in the concentration of protein and minerals, which usually are lower in the stem compared to the leaf. These differences are usually greater for tropical grass species than for temperate [12]. Thus NIR spectroscopy has been examined as a method to measuring the proportion of leaf present in the sample of the temperate grasses, tropical grasses and legume.

Oil

When it comes to mechanical components one valuable engineering tool is oil analysis. The goal is to prolong machine life and this can be done with assessment of component and lubricant condition. One of the main contaminants in lubricating oils is water. It accelerates the acid formation in the oil and can damage the component surface with its rapid expansion to steam especially in high pressure. The other important contaminants is diesel. This is usually present in the engine oil due to an injection failure. Diesel decreases both the viscosity and the film strength of the oil. This decreases the oil's ability to protect mechanical components from direct contact. According to study made in [13] it was possible to show that NIR spectroscopy is capable of quantifying water and diesel in unused engine, hydraulic and gear oils.

Wool

First NIR instruments for wool measured only residual grease level and moisture. Later when the spectral range was extended to cover both NIR and visible (Vis) regions it was possible to add colour measurement to the quality parameters. When it comes to the colour measurement the Vis-NIR instrument is capable of receiving wool from the coring instrument in a scouring plant. Base colour measurements are not only obtained but also "as is" colour values can be predicted. When wool is tested in commercial testing laboratories for measurement and certifications they test for things like residual materials which include the residual grease, mineral matter (which basically means the ash content) and vegetable matter [14]. Using these parameters the test yield is then calculated.

Paper

In the paper industry the measurement of moisture content is important because water is used to control many process properties. Just to name a couple of examples the absorption of water in the coating process and removal of it in the drying process. NIR spectroscopy is a good tool for moisture measurements and thus it is used in the paper industry because it offers fast and non-contact measurement. Furthermore, NIR spectroscopy technique is suitable for a large variety of basis weights. In ref. [3] it was shown that with NIR spectroscopic methods semi-quantitative moisture depth profiling in paper is possible.

2.5 Pharmaceutical processes

Lately near infrared (NIR) spectroscopy has become more popular amongst measuring and analysing samples in chemical industry. NIR spectroscopy is usually chosen for its speed and its low cost [15]. Also NIR spectroscopy does not destroy the analysed sample [16]. There are two different types of analyses that can be done by using NIR spectroscopy: qualitative analyses and quantitative analyses [15].

Qualitative analysis

Qualitative analysis is about classification of samples using their NIR spectra. There are different types of pattern recognition methods that one can use when

identifying the sample. Basically these methods can be divided into two different categories: the unsupervised and the supervised ones. In unsupervised classification there is no prior knowledge from the sample but only the gained spectra are used. In supervised classification, as one can guess, there is some knowledge about the sample beforehand, for example the measured spectra are compared to previously known spectra and the difference or the similarity of those spectra reveals information [15].

In supervised classification there are major differences between pattern recognition algorithms. They can be concentrated on discriminations or similarity between samples, parametric or non-parametric computations and linear or non-linear methods [15].

Quantitative analysis

When the classification of samples has been done logically the next point of interest is the extent of difference in the samples [15]. Parameters such as hardness, compaction force and dissolution rate can also be analysed quantitatively using NIR spectroscopy.

Online monitoring in pharmaceutical applications

The powder blending is a critical step in the manufacturing of pharmaceutical solid dosage forms. If the blend is not homogenous it is impossible to get the correct dose of active pharmaceutical ingredient in the tableting phase. The determination of blend homogeneity is a problem since samples are usually removed from the blender bin using a sample thief. Using this method causes changes in the distribution of the powder and when the sample is analyzed using some conventional chemical method the errors may come from the sampling [15]. Moreover, NIR spectroscopy can observe the most of or all constituents of the powder blend and not only the active pharmaceutical ingredient [17].

NIR spectroscopy can also be used when monitoring other important unit operations in manufacturing of pharmaceutical products like granulation, drying, cristallinity, coating and packaging [15].

3. Granulation

One of the reasons for granulation is that the tablets and capsules have become the most used solid dosage forms in medication. The tablet making process starts when the pharmaceutical ingredients are brought to the factory and the quality is checked. First, the correct amount of powder is measured then it is granulated and compressed to a tablet form. After this the tablet can be coated if necessary. Different pharmaceutical ingredients behave very cumbersome when it comes to compressibility and ability to form long-lasting briquettes. The solution for these problems is to use auxiliary substances and to shape the pharmaceutical ingredient mechanically [18].

Granulation itself is a process where primary powder particles are adhered to granules. There are reasons why granulation is often necessary [19]. *Improvement of the flow properties* is important because if the powders do not flow well it can result in a wide weight variation in the final product. *To prevent the segregation of the powder mix* is crucial especially when the amount of the pharmaceutical active ingredient is small. *The reducing of the dust* that may arise when handling powders comes to consideration when the powders are toxic [18]. Some powders are difficult to compact so the granulation is also used to *improve the compaction* of the mix.

3.1 Granulation methods

There are two different types of granulation methods: wet granulation and dry granulation. In the dry method no liquid is used but the primary powder particles are aggregated under high pressure. Two main processes of this are to squeeze the powder between two rollers to gain a sheet of material or to use a tablet press to produce a large tablet. Then the formed sheet or big tablet is crushed to smaller pieces which are then sieved to separate the desired size fraction. The

rest of the crushed material can be then processed further to avoid waste. If we look at the point of energy costs the dry granulation is not very economical method [18].

The most common granulation method is the wet granulation where dry powder mass is mixed with granulating fluid. This fluid contains a solvent, which is non toxic and can be removed by drying. The granulation fluid can consist only of the solvent or it can also have adhesive dissolved in it [19]. The most typical liquids are water, ethanol and isopropanol.

3.2 Wet granulators

There are three main types of wet granulators used in the pharmaceutical industry: shear granulators, high-speed mixer/granulators and fluidized bed granulators.

In the fluid bed granulator the powder particles are fluidized in a stream of air. The picture of a fluidized-bed granulator can be seen in Figure 7. First the powders are mixed in the container using air stream. Then the powder mass is sprayed with the granulating fluid and at the same time the air stream is still mixing the powders and making them move so that the liquid is spread evenly to the powders. The spraying happens through the nozzle situated over the bed of powders. Because of the granulating fluid the particles start to stick to each other and form granules. When the sufficient amount of granulation liquid is sprayed to the mix, then the nozzle is turned off and the hot air stream goes through the powders. This is the way the granules are dried. The advantage of the fluid bed granulator is that mixing, granulation and drying processes are performed in the same unit. This obviously saves time, transfer losses and labour costs. Furthermore, processes happen in a closed space so the inconvenience of dust is avoided.

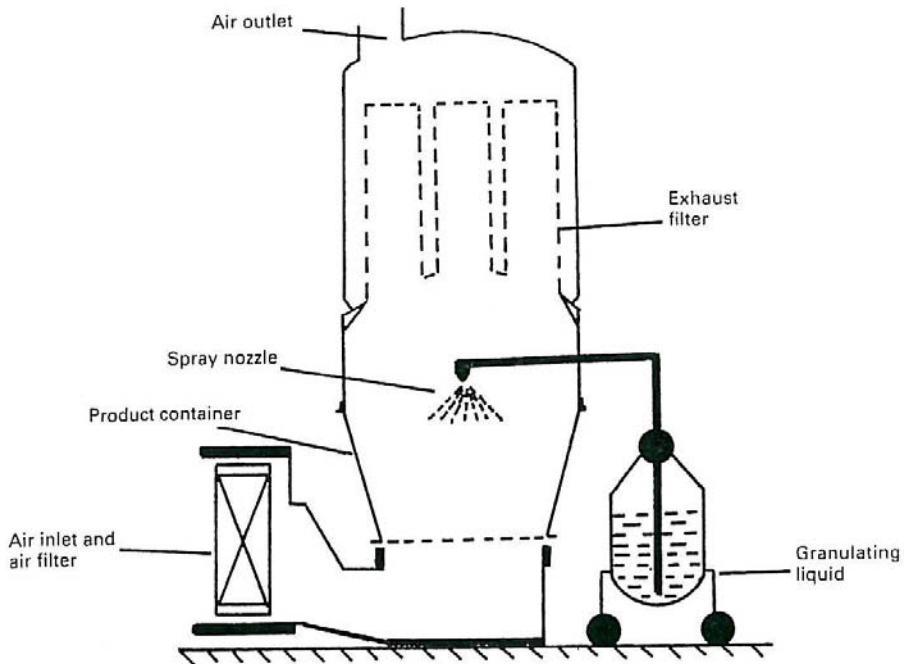

Figure 7. Fluidized-bed granulator [16].

In shear granulators the mixed powders are fed into the bowl of the planetary mixer. Then, the granulating liquid is added at the same time when the powder mass is mixed with the mixing arm. After mixing the moist mass is transferred to a granulator which forces the moist mass through a certain size of sieve screen. Then the last thing to do is the drying of the granules by collecting them to trays and transferring them to a drying oven. The tray drying has, however, three major disadvantages. The drying time is long, dissolved material can migrate to the upper surface in the bed of granules, and granules may aggregate at the points of contact of the granules. After drying it is important to sieve the mass again in order to remix and disaggregate the granules. The advantage of this whole process is that it is not very sensitive to changes in the characteristics of the granule ingredients.

In the high-speed mixer/granulator the unmixed dry powders are placed in a stainless steel mixing bowl and the powders are mixed by the rotating impeller for a few minutes. The granulating liquid is added through a port in the lid of the granulator and the rotating impeller is moving. When the moist mass is formed a chopper is turned on. It breaks up the wet mass and produces a bed of granular

material. When the satisfactory granule has been formed, the mass is transferred to a fluidized-bed dryer. The advantage of this system is that the mixing, massing and granulation are all performed within a few minutes in the same piece of equipment [19]. The whole process has to be monitored carefully in order to pinpoint the moment when a granule with desired properties has been attained.

4. Multipoint-NIR-measurement system and the performance tests of the system

The multipoint-NIR-measurement system and the performance tests are presented in this chapter.

4.1 Structure

The measurements of this work are done by a multipoint near-infrared measurement system. As one can see in Figure 10 on page 26 the system is basically constructed from a spectral camera, a fibre-optic light source, twelve probes and a computer. The fibres from the light source are connected to the probes and the collecting fibres leave from the probes to the actual spectral camera. The fibre connection panel makes it easier to connect the fibres to the spectral camera. In order to connect the fibres coming from the probes to the fibre connecting panel we need ST-ST connectors. The spectral camera is connected to the PC and to its controller. That way we can control for example the shutter of the spectral camera. A picture of the measurement system can be seen on Figure 8.

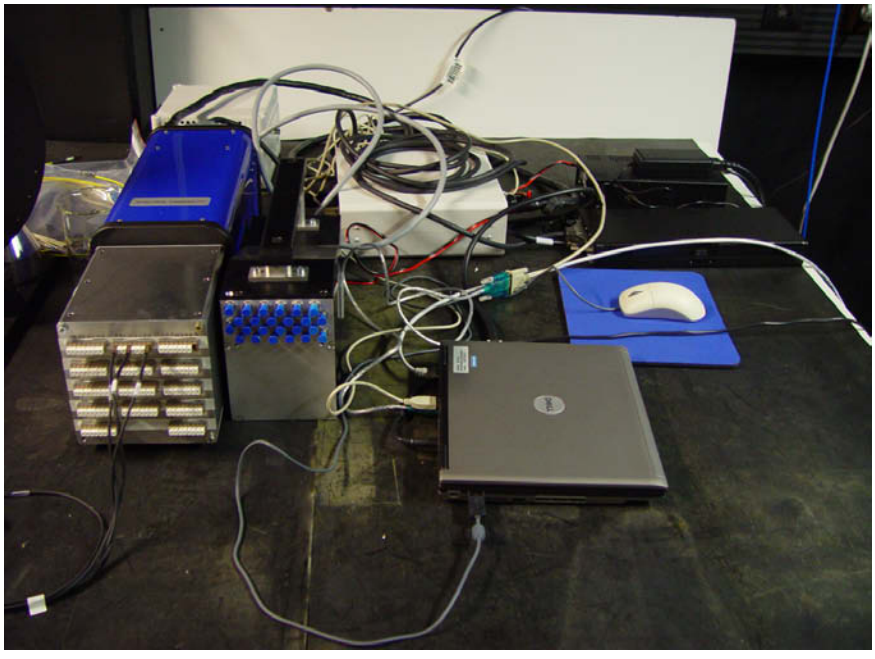

Figure 8. The multipoint-NIR-measurement system.

4.1.1 Light source

The used light source is more precisely a double-chopping fibre-optic light source with 24 output fibres. There are two fibre bundles, which means that there are two light paths. The chopper has one hole that is extending roughly one-third of the circumference. This means that the light path has three different possibilities: the light is coming through bundle 1, both bundles are dark or the light is coming through bundle 2. The light coming from the halogen bulb is collected to two mirrors situated at both sides of the bulb. The collecting mirrors form an image of the bulb to two imaging mirrors which in turn form the image of the collecting mirrors to the ends of two fibre-optic bundles. Just like in Figure 9 the chopper blade is situated between the imaging mirror and the fibre-optics bundle. The controller box includes a current source and some electronics that stabilises the bulb and controls the chopper. The controller maintains the resistance of the bulb stable which means that the temperature of the filament is stable too. The chopper also has a reading frame whose signal is used by the controller in order to keep the chopping frequency at desired level.

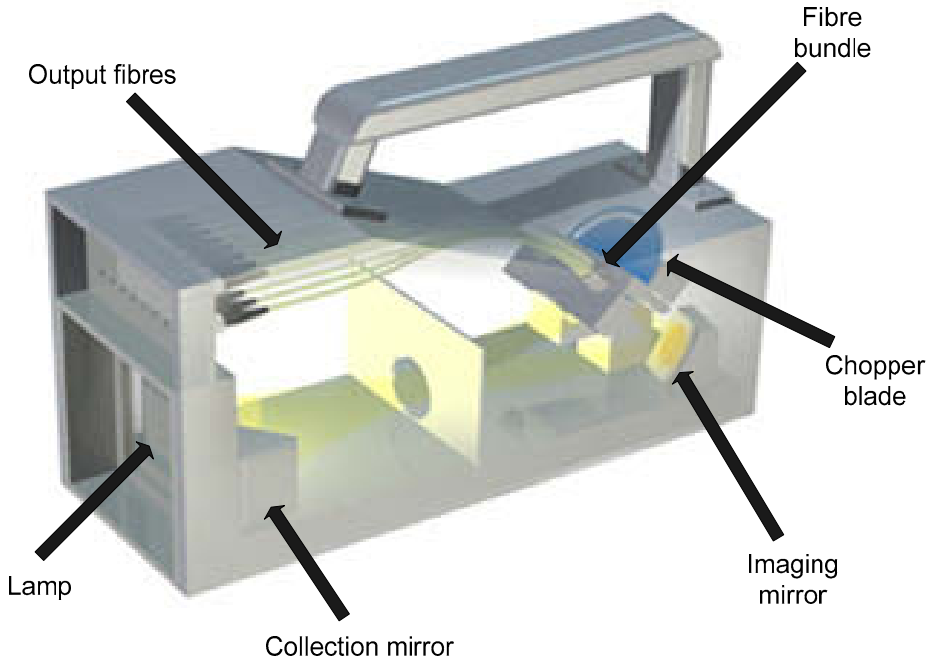

Figure 9. The fibre-optic light source.

4.1.2 Spectral camera

The used camera is a mercury-cadmium-telluride infrared camera, MCT camera for short. The camera has 253 rows and 320 columns, its spectral range is 968–2436 nm and it can take 100 frames in one second. The camera is cooled by a 4-stage Peltier cooler so the temperature can be as low as -80 degrees Celsius. The use of fibre-optic illumination in probes is possible because the MCT camera is a very sensitive instrument. It has 110 input fibres with core diameter 62,5 µm. This enables the measurement of 110 infrared spectra from different positions at the same time. The camera has a 14-bit analogue-to-digital converter. The camera is operated by software that has been developed by the vendor Specim Ltd. The software is used for grabbing of frames but it can not separate of the signal from the input fibres. All the rest data processing is done by custom-made MATLAB programs.

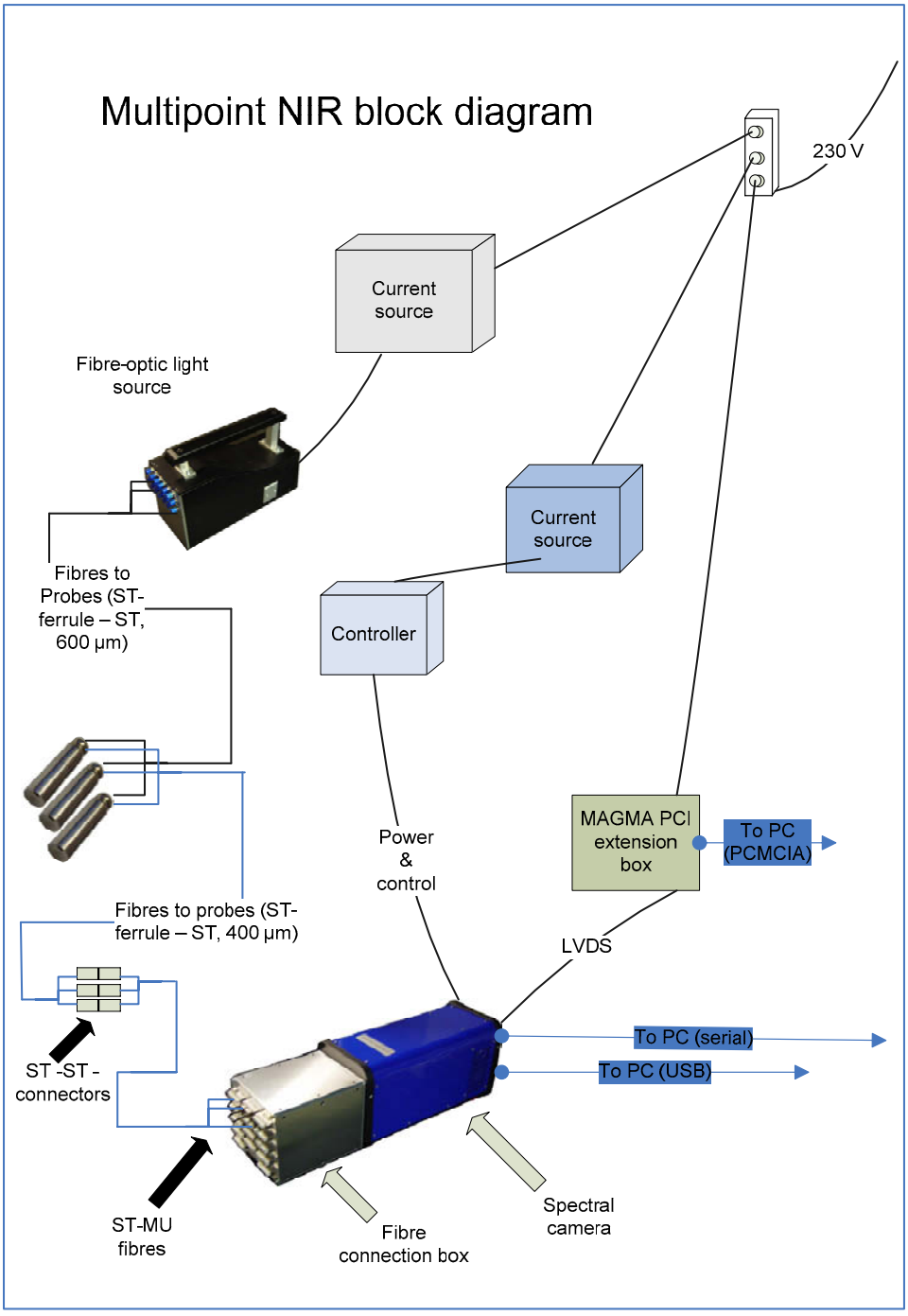

Figure 10. Multipoint NIR block diagram.

4.1.3 Probes and fibres

One illumination and collection fibre is situated inside a probe and there are 12 probes total. In Figure 11 we can see inside of one probe. The light coming from the illumination fibre is reflected from an ellipsoid mirror and then from a plane mirror to the sample outside of the probe. The plane mirror folds the optical path so that the ellipsoid mirror forms an image of the fibre end at the sample. Then the light reflects from the sample back to the probe and using another plane mirror and an ellipsoid mirror it reaches the collection fibre. After the plane mirrors there is a window and a revolving plate. The window is situated so that even if it gets unclean the only way it affects the measurement results is that the intensity gets a bit smaller. The revolving plate has two holes and one dark spot in it. Under one hole there is a mirror which is in 45 degree angle and when the light comes from the hole to the mirror it is reflected to a reference sample situated inside the probe. This makes it possible to measure the reference without taking any extra reference sample everywhere. The other hole is used when making measurements from the sample and the dark spot can be used when making a dark current measurement. In our measurement we use the shutter in the spectral camera when making the dark current measurement.

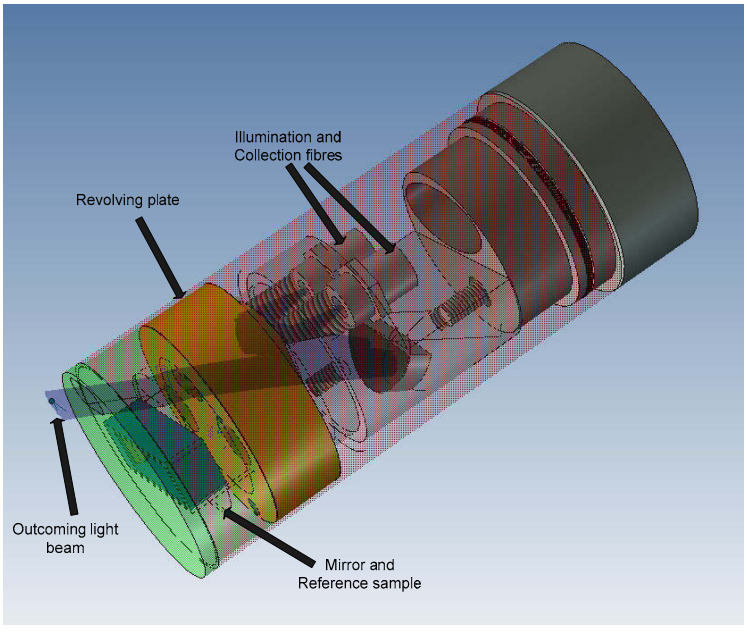

Figure 11. Optics inside the probe.

4.2 How does it work?

Using the computer we can control for example integration time, how many pictures are taken in a second and how many frames are captured. A shutter, that is located inside of the camera, is used when measuring the dark current. The area from where the probe can measure is located around 0 to 1,5 cm from the end of the probe. Any further than this separates the illumination spot from the collection spot.

Extracting the channels from the images is realised as follows. A single column in the image is occupied by one channel. The program works in a way that it reads the sequence of images and maps the appropriate columns to a matrix. This matrix is then saved. The x-axis is the spatial direction and the y-axis is the spectral direction. In Figure 12 there are eight channels that actually see something.

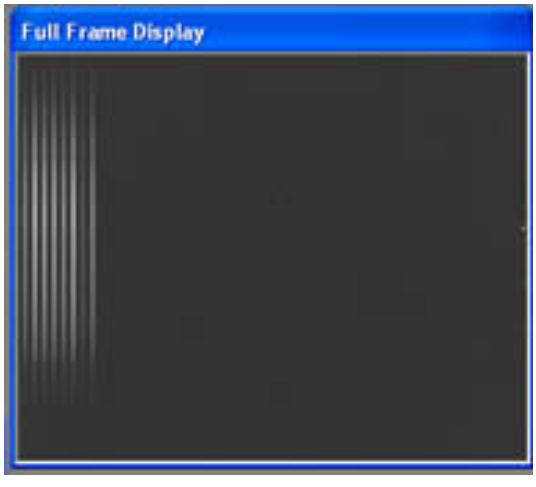

Figure 12. Measurement image collected by the spectral camera.

After performing the measurement the data is transferred to a MATLAB program and it is analysed there. The first thing to do is to transfer the raw data to MATLAB code so that it is possible to work with it. The absorbance is calculated from the measured data using the expression

$$X = -\log\left(\frac{I-D}{R-D}\right),$$

where X is the calculated absorbance, I is the measured sample, D is the dark current and R is the white reference. It is good to remember that X, D, R and I are in matrix form. This is the basic formula used when analysing the data.

4.3 Performance tests

Because the measurement system is so new, the first thing to do is make the performance tests. By these tests, we get information about probe-to-probe comparability, stability of the system and signal-to-noise ratio. Totally there are six different tests to make and results to analyse. In every test the white reference and dark current are also measured unless stated differently.

4.3.1 Signal-to-noise ratio

In signal-to-noise ratio measurement optical teflon (Gigahertz-Optik GmbH OP.DI.MA) was being used as a sample for all twelve probes. A thousand measurements were taken and signal-to-noise ratio was calculated. The SNR was calculated like the following

$$SNR = \frac{mean(I - D)}{std(I - D)},$$

where SNR is signal-to-noise ratio, I is the measured sample, D is the measured dark current, mean stands for the mean value and std stands for standard deviation. The results for SNR can be seen in Figure 13. As expected the SNR gained its maximum value around halfway of the measured wavelength region and deteriorated when moving higher or lower at the wavelength scale. This was because of the efficiency of the grating and the responsivity of the camera. The measured SNR was clearly over one as expected.

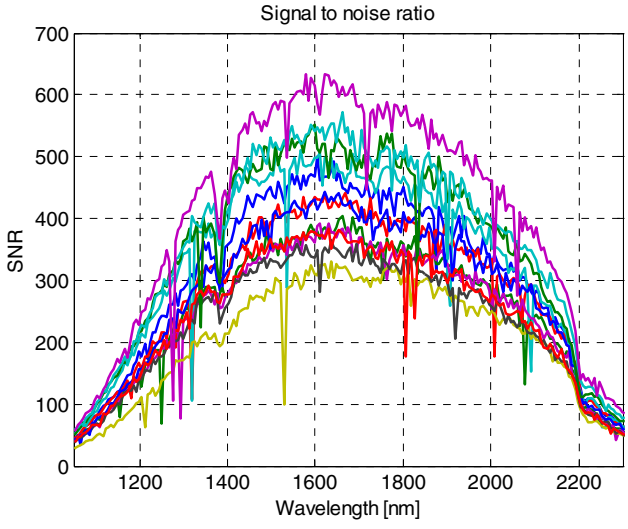

Figure 13. Signal to noise ratio using optical teflon as a sample.

4.3.2 Dark current stability

The dark current was measured for an hour and the spectral behaviour for all of the probes was calculated. The drifting of the dark current for four probes can be seen in Figure 14. As it can be observed the dark current doesn't change considerably during the measurement time. The spikes are the result of the bad pixels in the spectral camera. This sort of behaviour is normally fixed in the processing of the data.

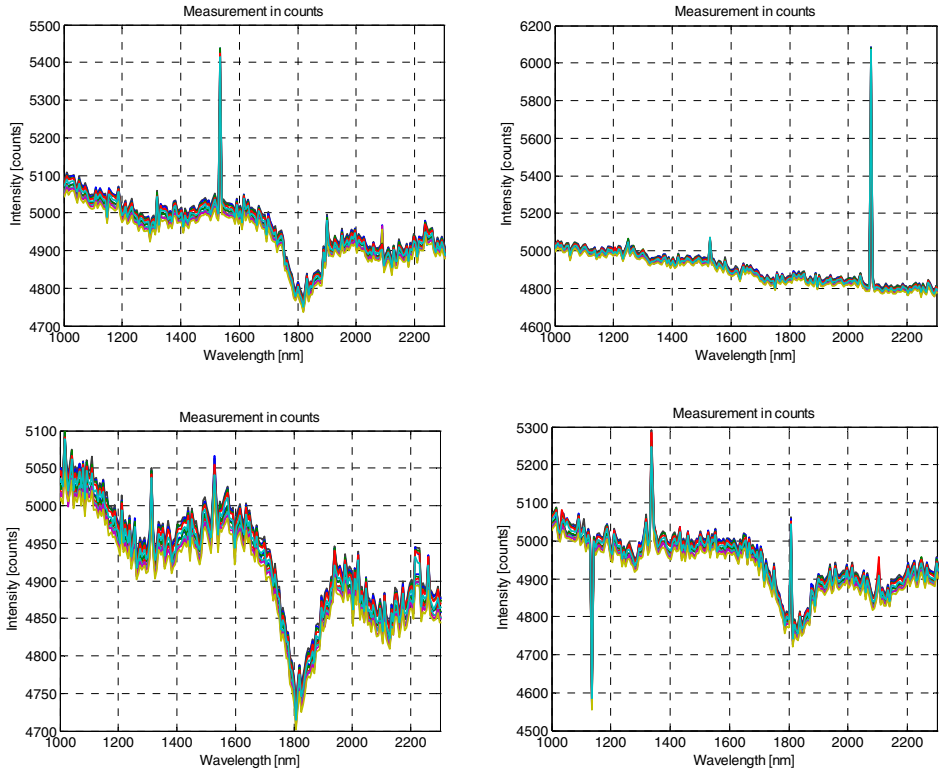

Figure 14. The dark current behaviour for four probes during one hour.

4.3.3 Long-term stability

There were two different types of measurements made when the long-term stability was studied. In both measurements optical teflon was used as the sample. First measurement took for an hour and a half. The results of this measurement were analysed separately to each probe. The measured time was divided into sequences and the first sequence was used as a reference for the rest, and the absorbance spectrum was calculated using Equation 1. The results of two probes can be seen in Figure 15.

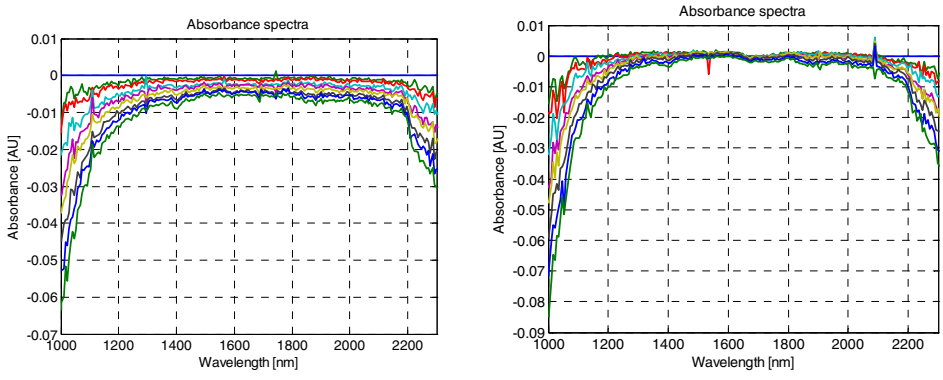

Figure 15. Absorbance spectra for an hour and a half long measurement for two probes.

The second measurement was a series of measurements measured once in an hour for seven times. It was constructed by repeating the same measurement for seven times so that there was an hour between two measurements. The first and last measurements as well as two measurements in between can be seen in Figure 16. The difference that can be seen is small and this tells us that the long term stability of the measuring system is quite good.

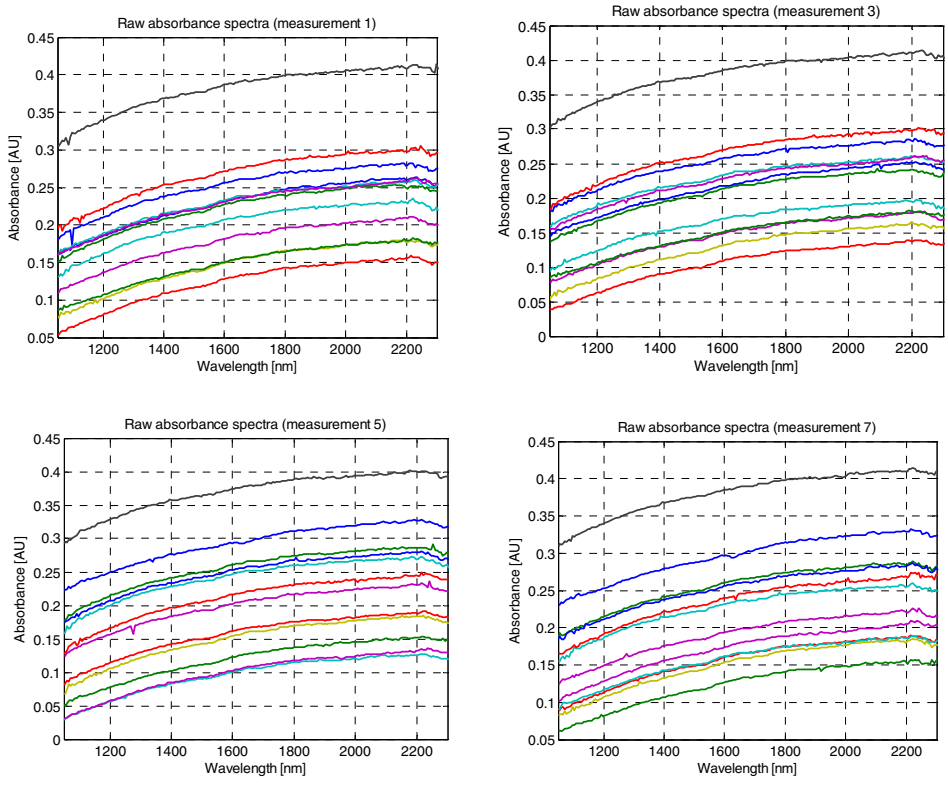

Figure 16. Once in an hour measured absorbance spectra. Measurements number 1, 3, 5 and 7.

The exact time when the white reference and dark current are measured might have a quite big impact on the measurement results. To see what kind of effect different measurement times have, we run our normal MATLAB routine using four different combinations of white reference and dark current measurement times. The decision to make different calculations for one probe only was made in order to make the pictures as clear as possible. First dark current and white reference measured once in an hour at the same time as the sample are used. Then the dark current and white reference measured at the beginning of the experiment for all seven sample measurements are used. In the third combination, the white reference measured at the beginning of the experiment and the dark current measured at the same time as the sample are used. And for the last combination the dark current that is measured at the beginning of the experiment and the white reference that is measured at the same time as the

sample are used. However, it is important to notice that for white reference the dark current measured at the same time is always used. The results can be seen in Figure 17. It can also be observed that as expected the best results are achieved by using the white reference and dark current measured at the same time as the sample. On the other hand, using the old reference deteriorates the results only slightly. Thus, it can be concluded that the dark current has to be measured frequently but the white reference not so often.

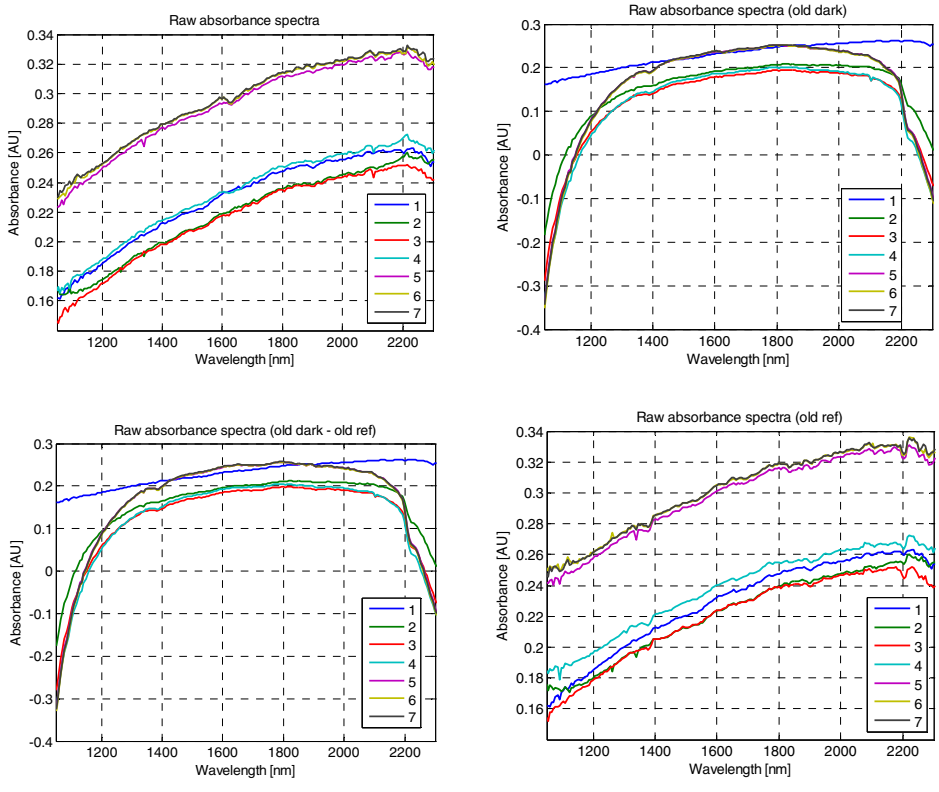

Figure 17. Raw absorbance spectra with different combinations of white reference and dark current for probe number 1.

4.3.4 White-reference repeatability

The white-reference repeatability was made with one probe. There were thirty consecutive white reference measurements made so that the probe was always turned to the measurement position in between the measurements. When

analysing the results, the first measurement was used as a reference measurement and the absorbance calculated. This way the difference between the measurements themselves can be seen. And as can be seen in Figure 18 the curve starts bending downwards at the sides of the picture, but in the middle measurements are nicely line shaped.

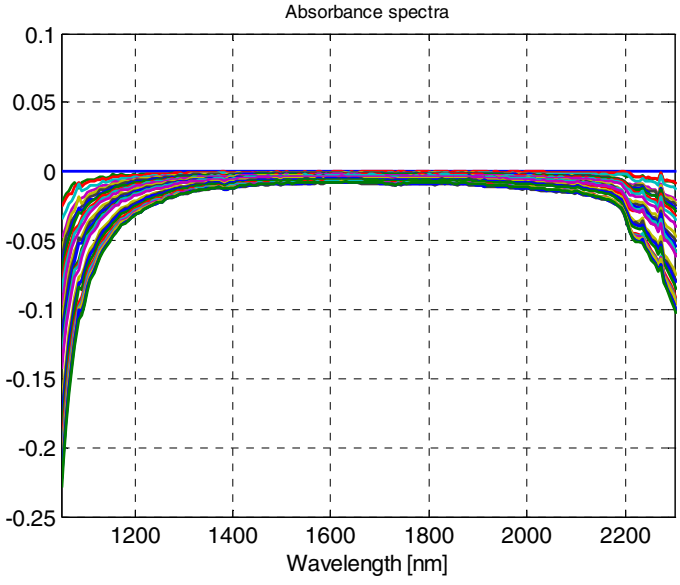

Figure 18. Absorbance spectrum for the white-reference measurement.

4.3.5 Probe-to-probe comparability

Probe-to-probe comparability is extremely important to measure. It can reveal whether the measurements made by different probes can be compared with each other and whether or not it matters which probe is used when making the measurements. The measurements were made using two different samples: optical teflon and polystyrene. The results can be seen in Figure 19 and we notice that the difference can be seen in absorbance spectra at the baseline level. The baseline shifts can be corrected using a technique which takes two different points or areas and fits the baseline of the data to this calculated level. When the baseline is corrected the difference between probes are small. This means that it is possible to use the probe that happens to be in the best measuring position when making the measurements and it is not necessary to worry about the result

being dramatically different from probe to probe. The good probe-to-probe comparability makes it possible to compare results from different probes to each other.

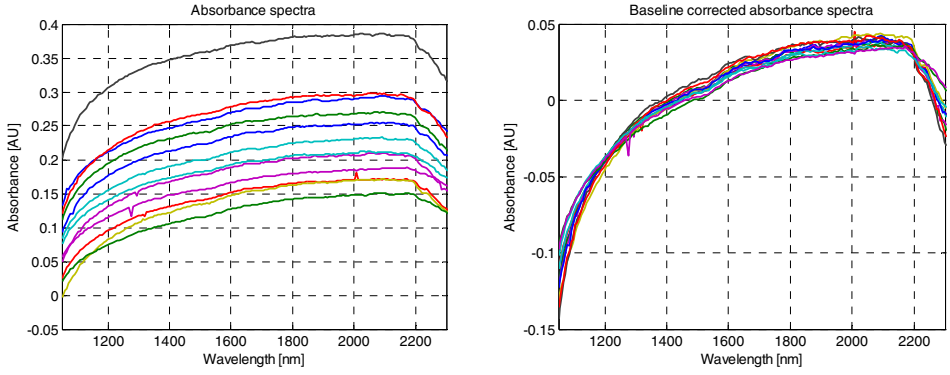

Figure 19. Raw absorbance spectra and baseline corrected absorbance spectra for optical teflon.

In Figure 20, we see the raw absorbance spectra for polystyrene. This spectra differs from the optical teflon spectra by having peaks in certain wavelengths. We see that the wavelength axis of the different probes is similar.

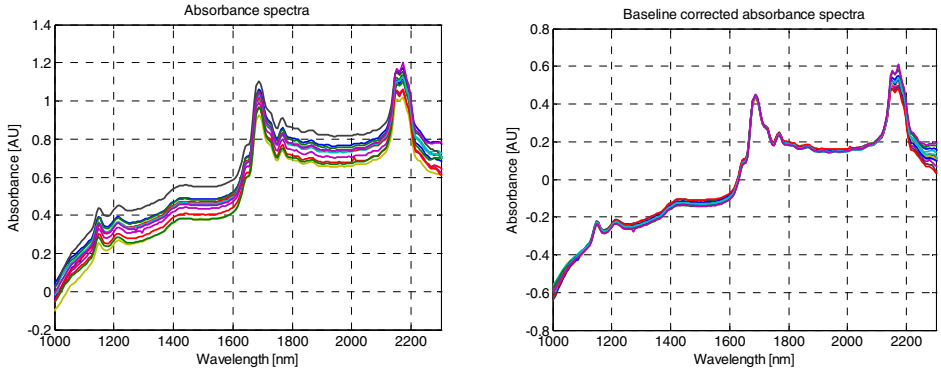

Figure 20. Raw and baseline corrected absorbance spectra for polystyrene.

4.3.6 Integration time dependence

The last performance test set was to study the influence of integration time on the spectra. As usual the sample was optical teflon, but now four different integration times were chosen: 1 ms, 2 ms, 5 ms and 10 ms. The dark current spectra for those chosen integration times are presented in Figure 21 and as expected the intensity increases when the integration time becomes longer.

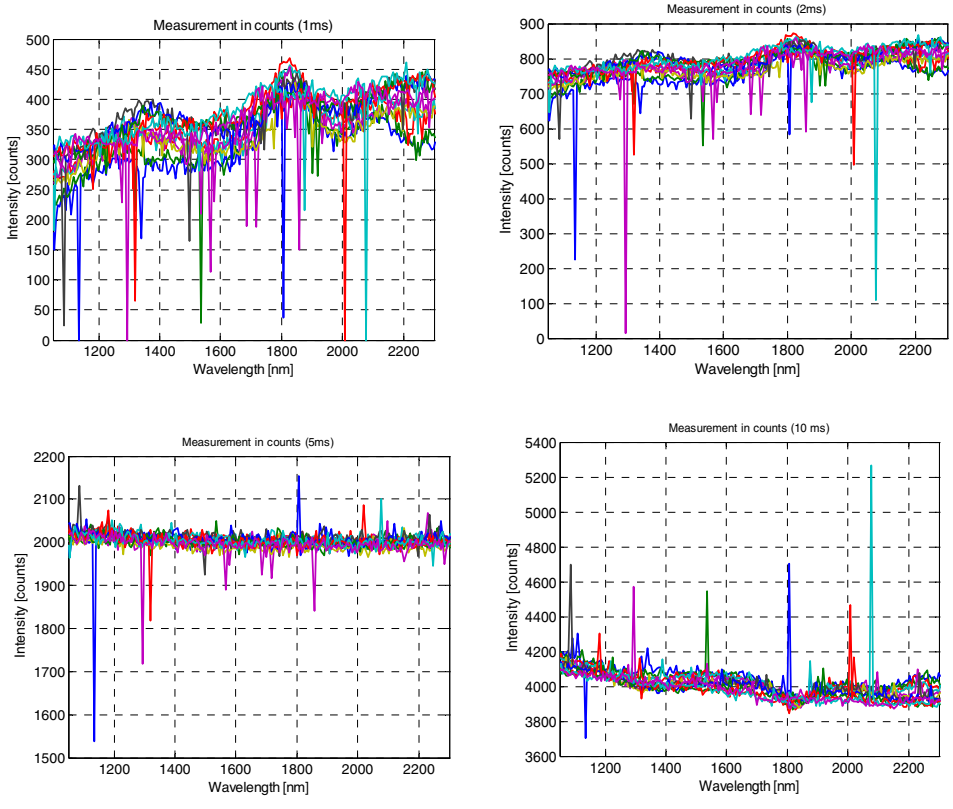

Figure 21. Dark current intensity spectra for different integration times.

The white reference was also measured and the results can be seen in Figure 22. Now some of the curves in the 10 ms integration time picture look a bit funny. This is because the spectral camera has reached its saturation limit but the real intensity is still higher than that border. This effect can also be seen in the absorbance spectra pictures of the optical teflon in Figure 23. Also this is the reason why integration time of 8 ms is so widely used in this work. The

absorbance spectra are similar to each other in the end of the spectra. This result means that there is no dependence on the integration time.

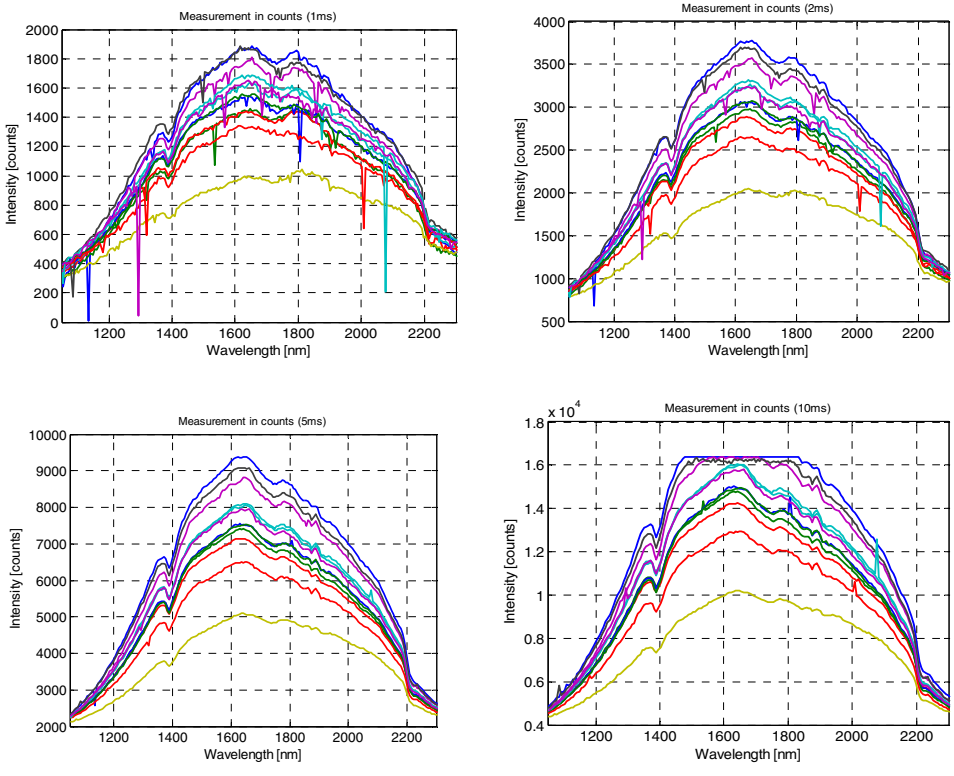

Figure 22. White reference intensity spectra for different integration times.

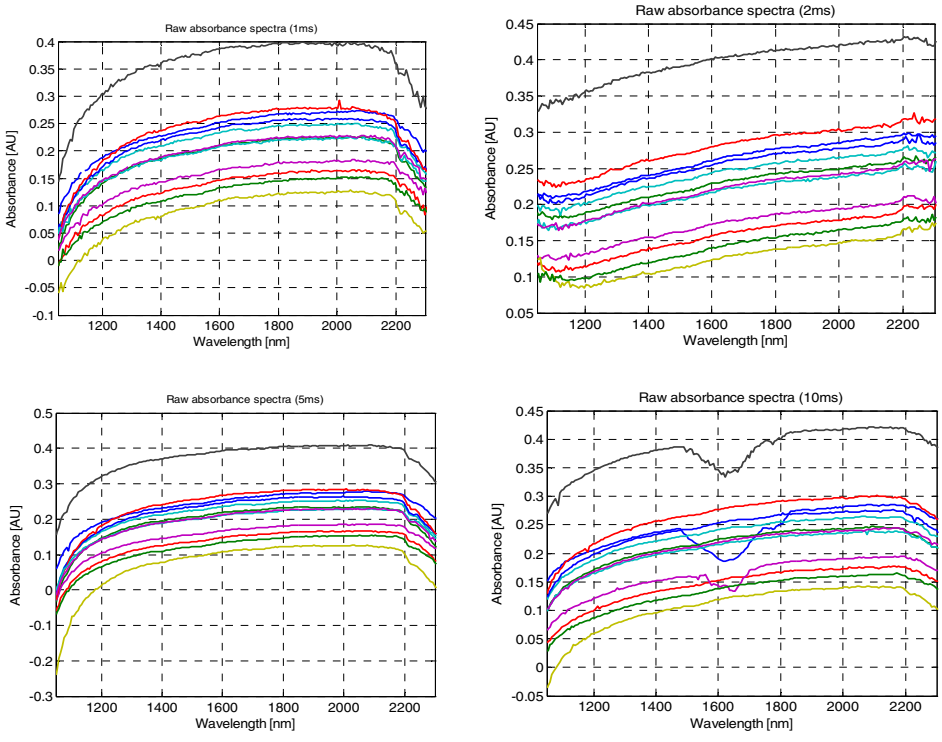

Figure 23. Raw absorbance spectra for different integration times using optical teflon as a sample.

4.4 Conclusion

The performance tests give a good ground to start working with this exact NIR measurement equipment. In later measurements, it is taken into account that it is possible to measure with all probes and the results will be comparable. The equipment can be turned on for longer periods of time and this does not affect the measurement results negatively. The only thing to be careful is to measure the dark current frequently enough. As a conclusion, these tests gives a good ground to start to make real process measurements and to analyse them.

5. Laboratory calibration sets

After performance tests it was time to make some off-line measurements in the form of calibration sets.

5.1 Samples

In the first laboratory calibration set we used lactose (granular size 200 M) and caffeine. Caffeine acted as active pharmaceutical ingredient. There were five samples in the calibration set such that the percentage of the pharmaceutical ingredient increased from 0% to 40% by steps of 10%. Also 1% of the total powder amount was a substance called polyvinylpyrrolidone (PVP or povidone) see Table 1.

Table 1. The percentage of the samples in laboratory calibration set of caffeine and lactose.

Sample	Lactose (%)	Caffeine (%)	PVP (%)
1	100	0	0
2	89	10	1
3	79	20	1
4	69	30	1
5	59	40	1

The PVP is acting as adhesive in the real mixing of powders so it was added to the calibration set too. Each of the powder blends were then mixed for 10 minutes with a mixer (Bioengineering inversina). The spectra of pure samples can be seen in Figure 24.

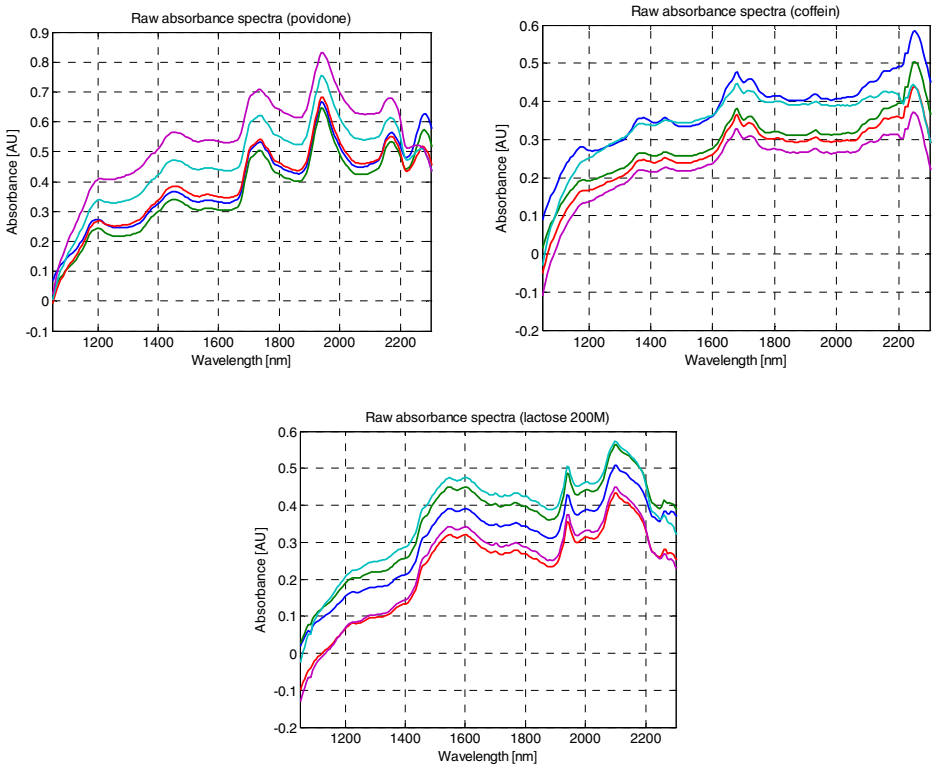

Figure 24. Raw absorbance spectra for pure samples.

The other calibration sets were made by the same procedure described above. In the other two calibration sets the pharmaceutical ingredient was ibuprofen mixed with two different granule size 50M and 125M of lactose. Here, as usual when it comes to granulation size, 50M granules are larger that 125M granules. This way the impact of the two different granule sizes can be observed.

Table 2. The percentage of the samples in laboratory calibration sets of ibuprofen and lactose. In one set the granule size is 50 M and in the other set 125 M.

Sample	Lactose (%)	Ibuprofen (%)
1	100	0
2	95	5
3	90	10
4	85	15
5	80	20
6	75	25
7	70	30

In these two sets the percentage of the pharmaceutical ingredient increased from 0% to 30% by the steps of 5% giving us total of 7 samples per granule size see Table 2. The spectra of pure samples can be seen in Figure 25.

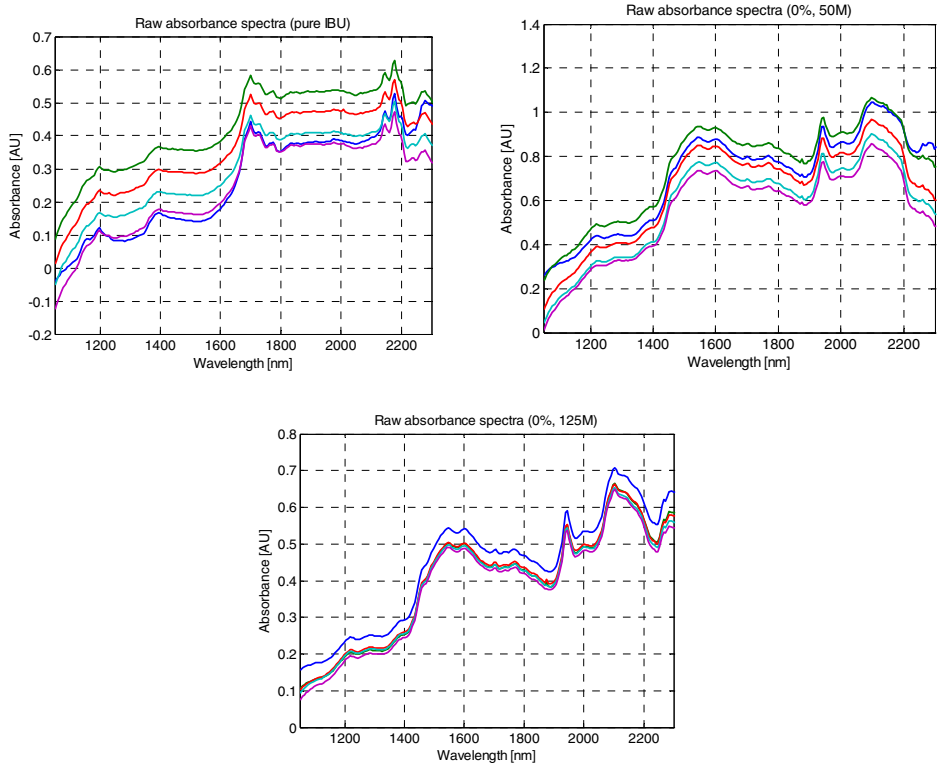

Figure 25. Raw absorbance spectra for pure ibuprofen and two types of lactose.

5.2 Measurements

The actual calibration set -measurements were made by placing the samples under wanted probes and making the measurements using the spectral camera. Used integration time was 8 ms and the camera took total of 1000 frames. Each sample was measured from five different positions.

5.3 Calibration models

Since the two main ingredients of the product in calibration set 1 are lactose and caffeine the end product spectra is a mixture between these two pure sample spectra. The main differences in the spectra between lactose and caffeine are the OH-peak (in lactose) height around 1900–2000 nm and the peak which exist in caffeine around 1700 nm. The mixed spectra for caffeine and lactose can be seen in Figure 26.

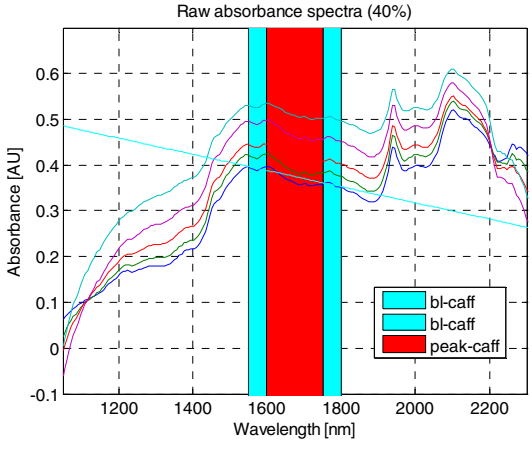

Figure 26. Mixed spectra for caffeine and lactose.

The mixed spectra for ibuprofen and two different lactoses are presented in Figure 27. The difference in ibuprofen and lactose spectra can be seen at the wavelength around 1700 nm.

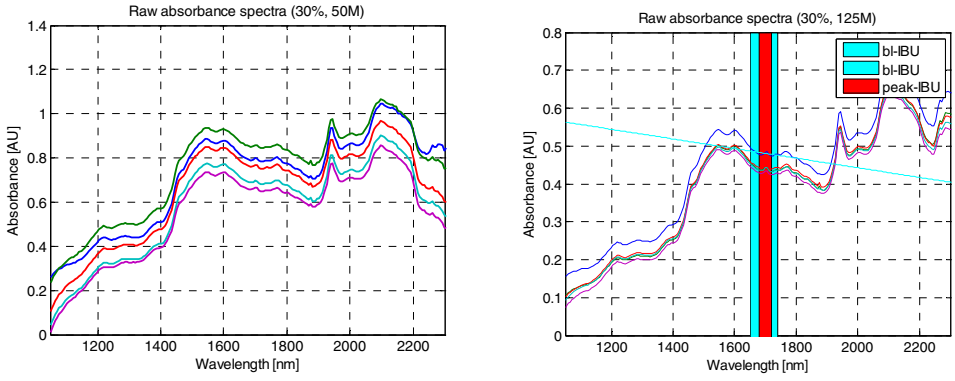

Figure 27. Mixed spectra for ibuprofen and lactose.

When making the most basic analysis on the set the area that differs in the pure samples is used. Normally this means that there is some sort of peak in other sample. Basically two points on both sides of the said peak is taken and a line is drawn through those areas. Then by integration the information about the area of the peak is achieved. The areas used for the baseline correction can also be seen in the pictures. These areas used for baseline in the case of caffeine are 1550–1600 nm and 1750–1800 nm and the peak integration area is 1600–1750 nm, see Figure 26. For the ibuprofen these areas are 1650–1680 nm and 1720–1740 nm for the baseline and for the peak 1680–1720 nm see Figure 26. In Figure 28 the peak high plotted with the caffeine and ibuprofen concentration can be seen. Furthermore a line is fitted into this data. The response is quite small, but enough to make the calibration. Note also that the response differs between the two granule size lactose.

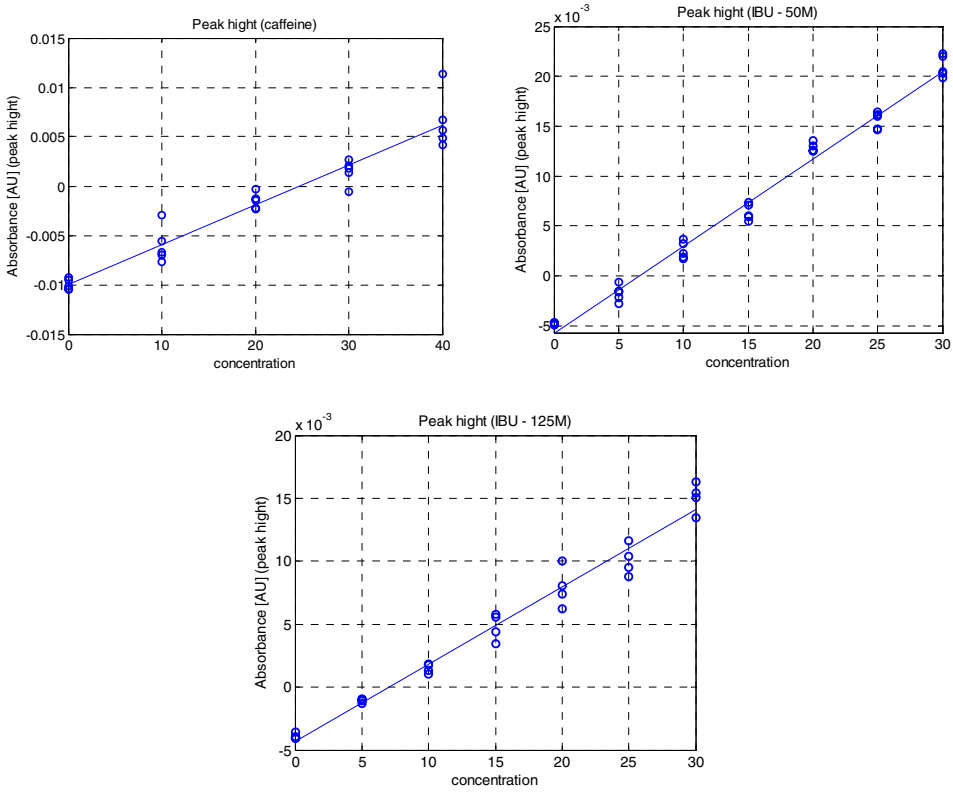

Figure 28. The relationship between the peak height and concentration.

Now it is possible to compare the prediction for the caffeine concentration to the actual amount of caffeine in the samples. Next make a scatter plot of predicted values versus reference values of the peak height for the caffeine. The explanation for the statistical information seen on scatter plot is as follows:

- *RMSECV:* root-mean-square error of cross-validation, this is an estimate for the one-sigma prediction error of the method;
- *cc:* the correlation coefficient between prediction and reference;
- *SECV:* the standard error of cross-validation (the same as RMSECV but the bias effect removed);
- *slope:* slope of straight line fitting of prediction vs. reference
- *offset:* offset of straight line fitting of prediction vs. reference

- *bias:* mean deviation of prediction from reference
- *CV:* coefficient of variability (CV = 100*standard error / mean of reference)
- *R2:* coefficient of determination which means the fraction of the total squared error that is explained by the model.

The R2 value can be calculated the following way

$$R2 = \frac{\mathrm{var}(Y) - \mathrm{var}(Y\_pred)}{\mathrm{var}(Y)},$$

where var means variance, Y is the reference concentration and Y_pred is the predicted concentration. As we can see in Figure 29 the coefficient of determination is 93,183%. One of the reasons this is not higher can be found in the inhomogeneity of the powder samples. Because the mixing was made in a way that the powders were just put together and then mixed instead of using some more sophisticated way the resulted powders may not be homogenous enough.

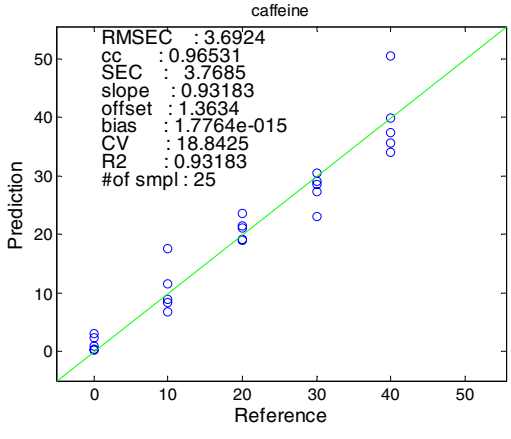

Figure 29. The prediction of the caffeine concentration.

As shown in Figure 30 the coefficients of determinations of the ibuprofen calibration are 98,616% and 97,295% depending on the granulation size of the lactose. In this case the powders were easier to mix due to the greater granulation sizes and the result is more homogeneous than the one with caffeine involved.

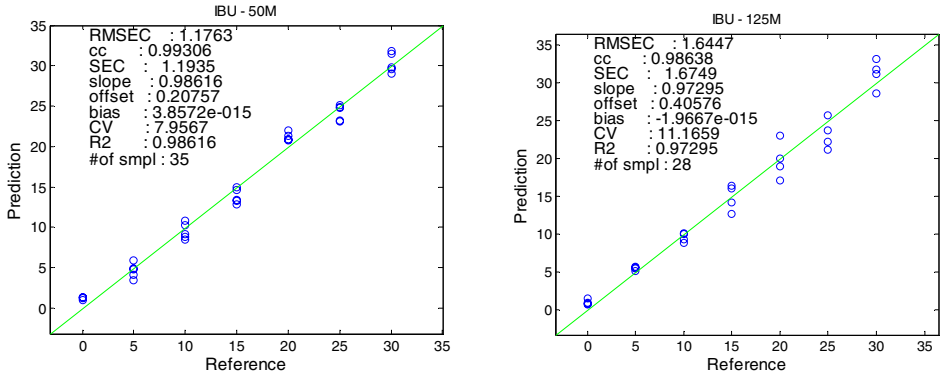

Figure 30. The prediction of the ibuprofen concentration.

Note that when the ibuprofen has the granule size of 125M the number of samples is only 28 compared to the 35 when the granule size is 50M. This is because the powder mass was not homogenous and one probe saw a big lump of ibuprofen. This effect can be seen when the peak high picture is plotted in the next Figure 31. Due to this that particular measurement was removed from the final analysis.

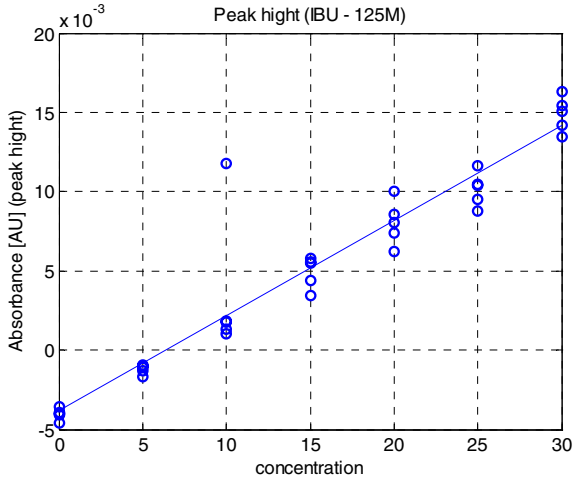

Figure 31. The relationship between the peak high and concentration before removing one measurement.

6. Fluid bed granulation

In the following chapter we will concentrate on the on-line measurements made from the granulation process. These measurements were made during September 2008 at the University of Helsinki.

6.1 Fluid bed granulator

The measurements were made by an AEROMATIC fluid bed granulator. The basic working idea is that in the beginning of the process the powders are put on the bottom of the container, which is then sealed. The air is pumped from the bottom of the container and it is going out from the top of the container. This air flow is responsible for the mixing of the powders as well as for keeping the powder mass from packing to the bottom. The nozzle situated on top of the container sprays chosen liquid to the powder mass at defined speed. Of course on top of everything else there are a lot of different sensors and ways to control the temperature, relative humidity, fan speed, pressure and pump speed. The actual NIR probes were attached to the granulator chamber in a way that can be seen in Figure 32.

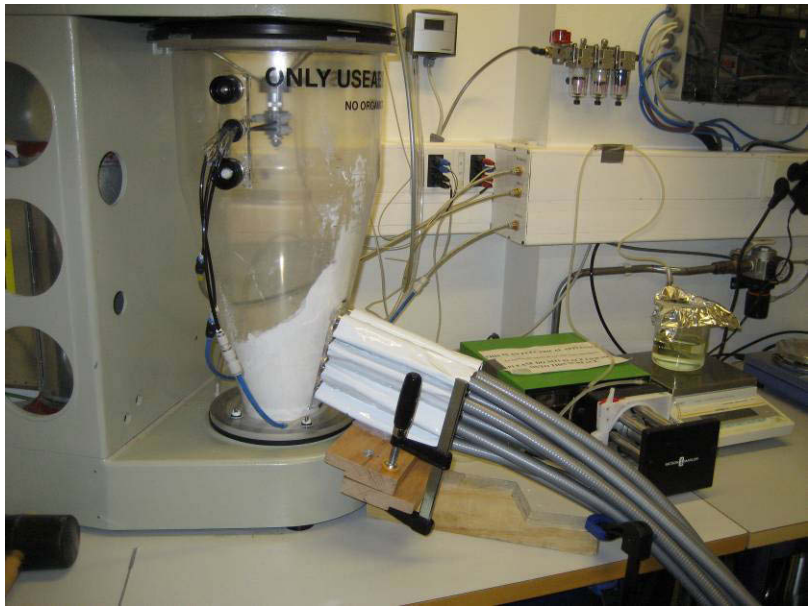

Figure 32. The fluid bed granulator.

6.2 Materials and methods

In the experiment, eight NIR probes were attached to the granulator. The arrangement order of the probes can be seen in Table 3.

Table 3. The order of the probes in the measurements.

probe 1	probe 2
probe 3	probe 4
probe 5	probe 6
probe 7	probe 8

A total of seven measurements were made with different type of air flow speed and two lactose granule sizes 80 M and 200 M. One measurement consisted of three different parts which were mixing, spraying and drying. The PVP was mixed with water and came in touch of the powders in the spraying phase. Sometimes depending on the mixed powders it is possible to use for example

only water in the spraying phase but in our case the PVP worked in a way as adhesive. The plan was to spray 100 g of the liquid mixture to the powder mass. When bigger granule size was used, none of the experiments went exactly like planned and were stopped earlier than designed. One basic measurement lasted about an hour while the recording frame speed was three frames per second. The used powders were lactose and caffeine and the mixing ration between those two was 80:20. The total amount of the powder mass was 800 g.

6.3 Results

The spectra for test number five in the beginning and at the end are presented in Figure 33. Here it can clearly be seen that the upper probes see only caffeine and the lower probes see only lactose in the beginning. This was how the powders were set out in the beginning of the test. The areas used for the baseline correction are also to be seen in the pictures. Note that the area used for caffeine is marked in the start spectra and the area used in water is marked in the end spectra. The peak area is in red and the baseline areas are coloured with turquoise. The peak formed around 1940 nm is the water peak [20]. The accurate baseline areas for the water peak were 1800–1876 nm and 1980–2025 nm. The area for the peak itself was 1920–1960 nm, and the area for the caffeine peak was 2222–2298 nm. Used baseline areas were 1490–1600 nm and 1976–2058 nm.

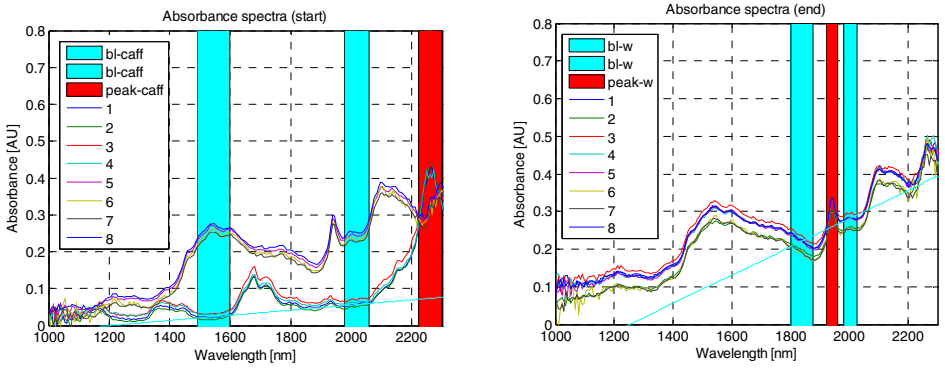

Figure 33. Starting and ending spectra.

6.3.1 Water peak

When calculating water peak height only every third frame is used because of the amount of the achieved data. In measurement one the result of water peak height calculation can be seen in Figure 34. The high and narrow peaks emerge when the probe sees an air pocket.

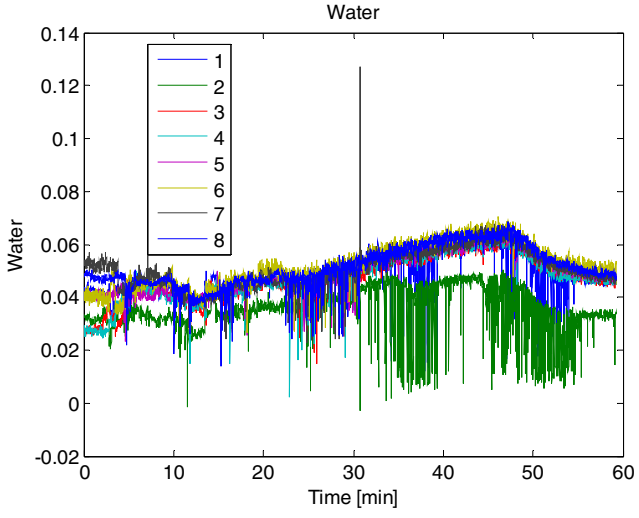

Figure 34. Water peak behaviour in measurement 1.

Now more data processing can be done by altering these voids out. These voids can be filtered. This means that regions of too high absorbance are cut off. Then these “bad” values are changed into interpolated ones, which are calculated using the nearest values. The results are then filtered by using a boxcar filter of width 10. After this process the new picture of measurement one can be seen in Figure 35. From now on the data is analysed like explained previously.

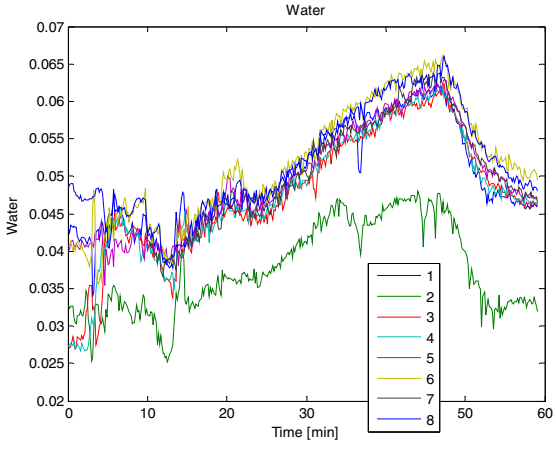

Figure 35. Water peak behaviour in measurement 1 after filtering.

The water peak measurement was successful in tests number one, five, six and seven. The results can be seen in Figure 36 below. When looking at the picture one should pay attention to the greater shapes instead of the bumpy behaviour of the lines.

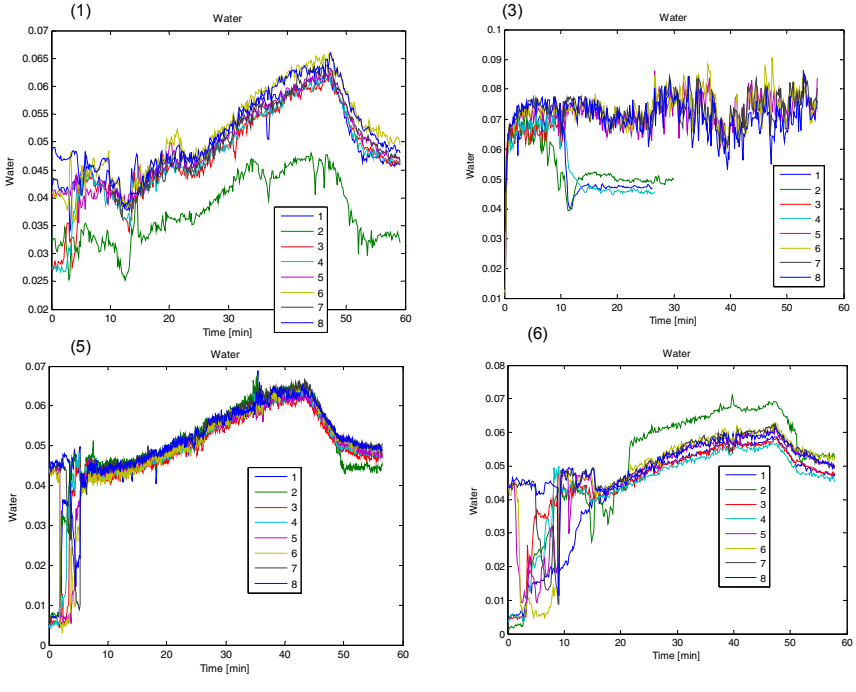

Figure 36. Water peak behaviour in measurements 1, 3, 5 and 6.

Picture number two in Figure 36 is an example of what an unsuccessful measurement looks like. In this case a wet spot was formed inside the chamber. When looking at the figure above, especially in pictures one and three, the three different states of the granulation process can clearly be seen. In the mixing phase the water peak is basically just a mess since the lactose itself has some hygroscopic water in it when caffeine does not have it. During the spraying phase the water peak grows steadily and in the drying phase the water peak goes down almost exponentially.

6.3.2 Caffeine peak and mixing

The caffeine peak was the other peak monitored. And there are two different things to be seen in the caffeine peak: the mixing and the effect of the granule size. The caffeine peak measurement was successful in measurements four, five, six and seven. The results can be seen in Figure 37.

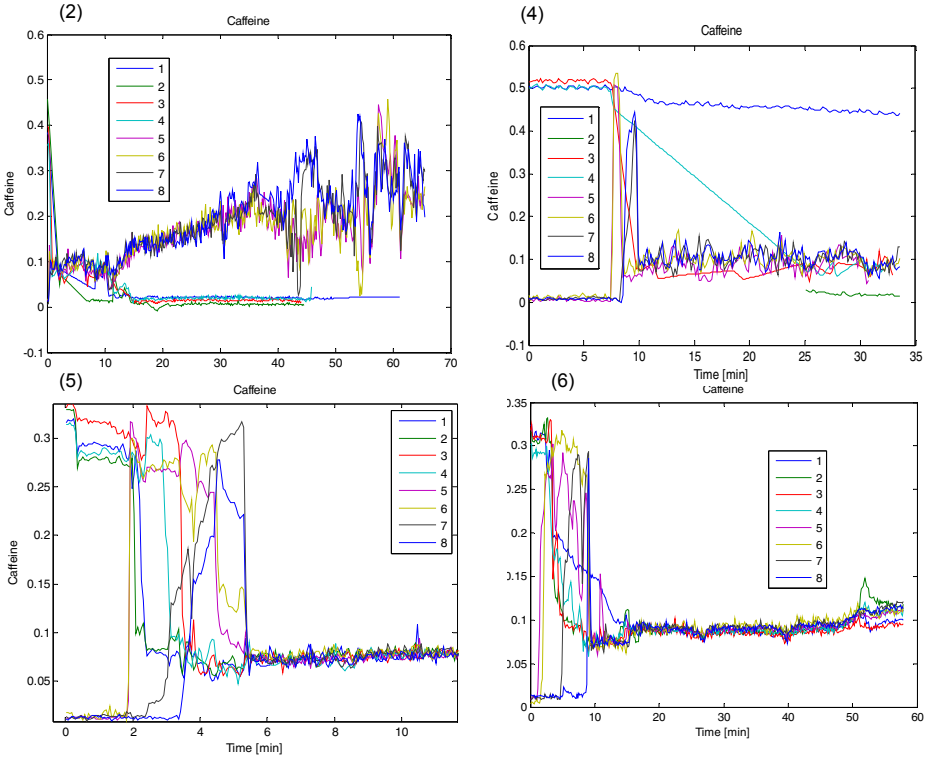

Figure 37. Caffeine peak behaviour in measurements 2, 4, 5 and 6.

Note that the first picture is from measurement two. It is clear from the picture that this measurement was not successful. In this measurement the particle size was larger and this made it more difficult to control the process. Even thought the plan was to spray 100 g of water and PVP mix we managed to spray only 90 g. The experiment had to be interrupted because too big lumps had formed at the bottom of the granulation chamber. Picture of the lumps can be seen in Figure 38.

Figure 38. Formed lumps at measurement two.

The powders were put to the granulator so that upper channels saw caffeine and lower ones saw lactose. Looking at the first picture in Figure 37 it is obvious that one of the probes has seen only caffeine during the whole measurement. The most natural explanation for this is the fact that there has been a caffeine spot stuck on the glass in front of the probe.

Also in the pictures two and three it can be seen that the caffeine curve is slightly increasing. This can be because the granulation size increases in the granulation process, which interferes the NIR measurement.

The mixing process of the experiments four, five and six can be seen more clearly in Figure 39. In the first picture the curves of two of the highest probes have been removed in order to see the mixing more clearly.

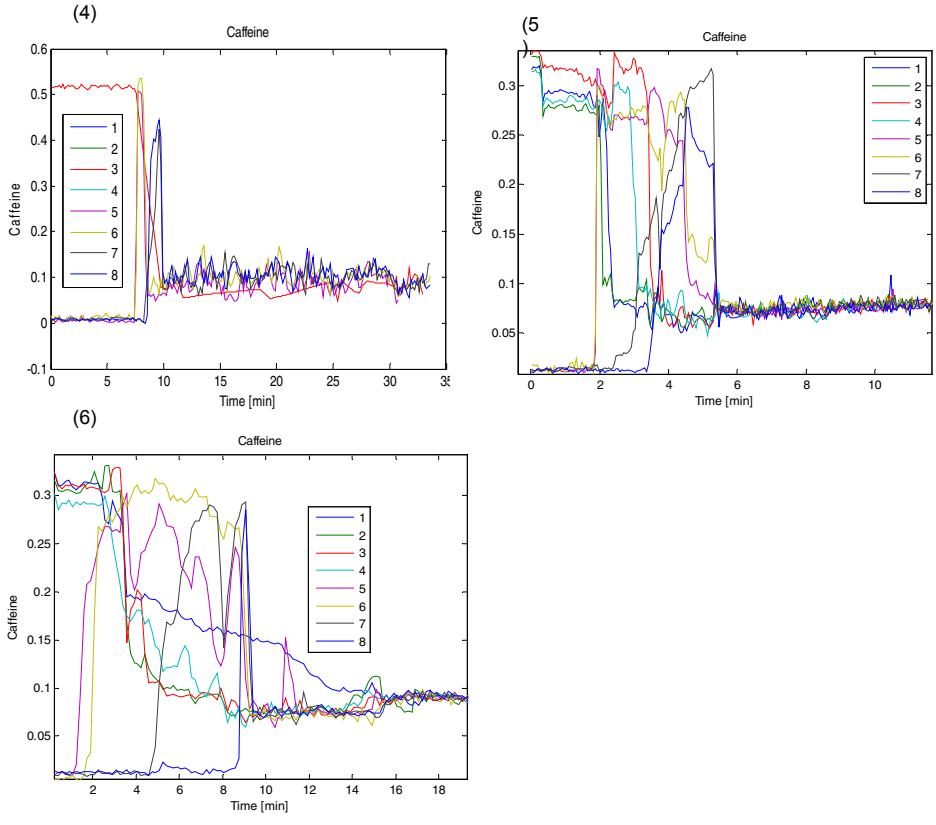

Figure 39. Caffeine peak behaviour in measurements 4, 5 and 6.

As can be seen the mixing process happens such that probes 1–4 are first on a high level and then drop suddenly. At the same time probes 5 and 6 jump up, after a while probe 7 jumps up and then finally probe 8.

To our knowledge, this kind of measurements have not been performed earlier on the fluid-bed granulation process.

7. Conclusions and summary

The aim of this work was to test the multipoint-NIR-measurement system both off-line and in on-line situations. The off-line measurements were made at VTT Oulu and the on-line measurements at the division if pharmaceutical technology of Helsinki University. All of these measurements were made during the year 2008.

Furthermore, the goal was to see whether the system works and for example if the probes are comparable. The work was started by making the needed performance tests. The multipoint-NIR-measurement system used was basically already designed and used except the addition of the probes themselves. Probe-to-probe comparability was found good meaning that it does not matter which probe is used at which place to make the measurements. The other important parameter is the signal to noise ratio. The SNR is largest in the region from 1500 nm to 1800 nm varying from probe to probe but in the best case it reaches over 600. Long-term stability was also good.

After the performance tests, the calibration sets for ibuprofen and caffeine were made. These gave the first implications that it is possible to measure difference between compounds. Also difference was seen when the percentage of the pharmaceutical ingredient was increased. After data analysing the predictions from these data was calculated. The coefficients of determination were over 90% in the case of caffeine and over 95% in the case of ibuprofen. Still it is good to keep in mind that despite of the mixing process the powders were not necessarily homogeneous. The thing to learn from these calibration sets it at least that different powder mixes require their own calibration sets.

The on-line measurements were made with caffeine and lactose mix. Moisture and mixing, in the form of the caffeine peak behaviour, were calculated from the data. When the granulation process was successful the moisture peak showed all three phases, which were mixing, spraying and drying. The powders were loaded

to the chamber so that the lactose was on the bottom and the caffeine was on top. From this setting the mixing could also be seen. The effect of the granule size on NIR signal could also be observed in the high of the baseline. This kind of multipoint NIR measurements have not been reported earlier in the literature. Thus, this thesis represents a pioneering work in this area.

In all, the multipoint NIR measurement device is fairly easy to set up on different measurement locations. Furthermore the multipoint measurement can be handled with just one spectral camera and the measurement can be done without destroying the sample itself. When making this type of measurements it is important to keep the window in front of the probes clean, because NIR spectroscopy does gather information only from the top layers. So, if the window is not clean, all the probes see is the layer on the window and not what is happening in the process itself. When something like that happens it is possible to just drop the data received from a probe that does not follow the actual process.

References

[1] Burns, D.A. and Ciurczak, E.W. (Eds.) *Handbook of Near-Infrared Analysis. Practical spectroscopy series, Vol. 13*, Marcel Dekker, New York, 1992.

[2] Herzberg, G. *Molecular spectra and molecular structure II Infrared and Raman spectra of polyatomic molecules.* D. Van Nostrand Company, Inc., Princeton, New Jersey, 1945.

[3] Paaso, J. *Moisture depth profiling in paper using near-infrared spectroscopy.* VTT Publications 664, Espoo, 2007. 193 p. + app. 6 p.

[4] Rantanen, J., Lehtola, S., Ramet, P., Mannermaa, J.-P. and Yliruusi, J. *On-line monitoring of moisture content in an instrumented fluidized bed granulator with a multi.channel NIR moisture sensor.* Powder technology, Vol. 99, No. 2, 1998, pp. 163–170.

[5] Townes, C.H. and Schawlow, A.L. *Microwave spectroscopy.* McGraw-Hill Book Company, Inc., New York, 1955.

[6] Siesler, H.W., Ozaki, Y., Kawata S. and Heise H.M. (Eds.) *Near-Infrared Spectroscopy: principles, instruments, applications.* Wiley-VHC, Weinheim, 2002.

[7] Chalmers, J. and Griffiths, P. (Eds.) *Handbook of vibrational spectroscopy. Vol. 1*, John Wiley & Sons, Chichester UK, 2002. Pp. 383–467.

[8] Känsäkoski, M., Kemppainen, A., Suhonen, J., Malinen, J., Rantanen, J., Yliruusi, J., Luostarinen K. and Nauha, P. *Integrated multichanel detector analysers at process control.* Near Infrared Spectroscopy: Proceedings of the 11th International Conference, Cordoba, Spain, NIR Publications, 2004. Pp. 121–126.

[9] Chalmers, J.M. and Griffiths, P.R. (Eds.) *Handbook of vibrational spectroscopy. Vol. 5 – Applications in Life, Pharmaceutical and Natural Sciences,* John Wiley & Sons Ltd, Chichester UK, 2002.

[10] Meyers, R.A. (Ed.) *Osborne, B.G. Near-infrared Spectroscopy in Food Analysis.* John Wiley & Sons Ltd, Chichester.

[11] Woodcock, T., Downey, G. and O'Donnell, C.P. *Review Better quality food and beverages: the role of near infrared spectroscopy.* Journal of Near Infrared Spectroscopy, 16, 2008, pp. 1–29.

[12] Dixon, R.M. and Zhu, G. *Measurement of the least content of tropical grasses with near infrared reflectance spectroscopy.* Near Infrared Spectroscopy 12th International Conference, 2005. Pp. 379–400.

[13] McArthur, L., Smitg R. and Greensill, C.J. *Quantification of water and diesel in lubricating oils using near infrared spectroscopy.* Near Infrared Spectroscopy 12th International Conference, 2005. Pp. 452–457.

[14] Ranford, S.L., Ellery, M.W. and Walls, R.J. *Specification of wool products using visible and near infrared analysis systems.* Near Infrared Spectroscopy 12th International Conference, 2005. Pp. 480–485.

[15] Roggo, Y., Pascal, C., Maurer, L., Carmen, L.-M., Aurélie, E. and Nadine, J. *A rewiew of near infrared spectroscopy and chemometrics in pharmaceutical technologies*. Journal of Pharmaceutical and Biomedical Analysis 44, 2007, pp. 683–700.

[16] Benedetti, C., Abatzoglou, N., Simard, J.-S., McDermott, L., Léonard, G. and Cartilier, L. *Cohesive, multicomponent, dense powder flow characterization by NIR*. International Journal of Pharmaceutics, 336, 2007, pp. 292–301.

[17] Kuhn, J., Korder, S., Arduini-Schuster, M.C., Caps R. and Fricke J. *Infrared-optical transmission and reflection measurements on loose powders*. Rev. Sci. Instrum., Vol. 64, No. 9, 1993, pp. 2523–2530.

[18] Juslin, M., Marvola, M., Paronen, P., Turakka, L., Urtti, A. and Ilkka, J. (Eds.) *Farmasian teknologia*, Farmasian opiskelijayhdistys Fortis Kuopio, 1990.

[19] Aulton, M.E. (Ed.) *Pharmaceutics the Science of Dosage Form Design*. Churchill Livingstone, 2002. Pp. 364–378.

[20] Hale, G. and Querry, M. *Optical Constants of Water in the 200-nm to 200-μm Wavelength Region.* Applied Optics, Vol. 12, 1973, pp.167–173.

Series title, number and report code of publication

VTT Publications 704
VTT-PUBS-704

Author(s)
Anne Heikkilä

Title

Multipoint-NIR-measurements in pharmaceutical powder applications

Abstract

In this paper, multipoint near-infrared (NIR) spectroscopy is used in studying particulate pharmaceutical ingredients and their mixing and granulation processes. Homogeneous mixing of active pharmaceutical ingredients with excipients is essential in getting the correct dosage in the tableting phase. The basic principles of NIR spectroscopy and the associated molecular vibrations are briefly reviewed in the beginning of the work, followed by a summary of typical applications of NIR spectroscopy.

A multipoint NIR measurement system developed at VTT is presented in this work. It consists of a spectral camera with fiber-optic inputs, a fiber-optic light source and twelve fiber-optic probes. The performance of the system in the laboratory is thoroughly reported, including signal-to-noise ratio, stability and probe-to-probe variability. The system was also tested in a fluidized bed granulator at Helsinki University. Eight probes were attached in two rows into the granulator, and several granulations were run. The mixing period in the beginning of the granulation process was clearly visible, as well as the changes in the moisture level during liquid spraying and final drying. The study shows that multipoint NIR spectroscopy is a valuable tool in monitoring the granulation process. In particular, it gives information about the macroscopic homogeneity of the fluidized bed.

ISBN
978-951-38-7334-9 (soft back ed.)
978-951-38-7335-6 (URL: http://www.vtt.fi/publications/index.jsp)

Series title and ISSN
VTT Publications
1235-0621 (soft back ed.)
1455-0849 (URL: http://www.vtt.fi/publications/index.jsp)

Project number

Date
January 2009

Language
English

Pages
59 p.

Name of project

Commissioned by

Keywords
pharmaceutical powder applications, fluid bed granulation, on-line monitoring, moisture content, mixing end-point, near-infrared spectroscopy, NIR, multichannel spectroscopy, fibre-optic probes, fibre-optic light sources, multipoint-NIR

Publisher
VTT Technical Research Centre of Finland
P.O. Box 1000, FI-02044 VTT, Finland
Phone internat. +358 20 722 4520
Fax +358 20 722 4374

VTT PUBLICATIONS

ISBN 978-951-38-7334-9 (soft back ed.)
ISSN 1235-0621 (soft back ed.)

ISBN 978-951-38-7335-6 (URL: http://www.vtt.fi/publications/index.jsp)
ISSN 1455-0849 (URL: http://www.vtt.fi/publications/index.jsp)